Ecological Informatics 95 (2026) 103736

Contents lists available at ScienceDirect

Ecological Informatics

journal homepage: www.elsevier.com/locate/ecolinf

# Individual-based modelling of small pelagic fish in the Adriatic Sea: integrating stock assessments, ecophysiology of fish, and environmental forcings

E. Donati [a,b,*], N. Marn [c,d], I. Haberle [e,f], S. Libralato [a]

[a] National Institute of Oceanography and Applied Geophysics-OGS, Section of Oceanography, Trieste, Italy
[b] Department of Life Sciences, University of Trieste, 34127 Trieste, TS, Italy
[c] Division for Marine and Environmental Research, Ruđer Bošković Institute, HR-10002 Zagreb, Croatia
[d] UWA Oceans Institute and School of Biological Sciences, University of Western Australia, 6009 Perth, WA, Australia
[e] Center for Marine Research, Ruđer Bošković Institute, 52210 Rovinj, Croatia
[f] Department of Biological Sciences, Florida Atlantic University, Boca Raton, FL 33431, USA

## ARTICLE INFO

*Keywords:*
*Anchovy*
*Sardine*
*Dynamic energy budget*
*Population dynamics*
*Agent-based modelling*

## ABSTRACT

Understanding population dynamics requires linking individual-level physiology to emergent population patterns. This study presents the first application of a dynamic energy budget individual-based model (DEB-IBM) to European pilchard (*Sardina pilchardus*) and European anchovy (*Engraulis encransicolus*) populations in the Adriatic Sea. The SPelAgent modelling framework, implemented in the Julia programming language, simulates fish energy acquisition and allocation throughout the life cycle as a function of environmental conditions, while prioritising simplicity in model structure and assumptions.

To hindcast past population trajectories in the Adriatic Sea, SPelAgent is forced with temperature and zooplankton time series from physical and biogeochemical reanalyses, and informed with age-specific fishing and natural mortality from stock assessments. SPelAgent captures energy allocation patterns, reproductive rates and size at puberty, although it overestimates the growth of sardine and older anchovy specimens; this could be improved through region-specific parameterisation. Model outputs qualitatively reproduce trends in catch data and stock-assessment biomass estimates, but their accuracy is limited by the need to control unrealistic population dynamics arising from simplified individual processes. The resulting differences in population structure between SPelAgent and the stock assessment lead to inconsistent outcomes when applying fishing mortality estimated from the stock assessment. This highlights the importance of explicitly representing prey dynamics and modelling fishing mortality within the model context. Overall, the model offers a mechanistic approach to studying small pelagic fish demography, accounting for individual variability and climate-driven effects on population dynamics, while prioritising simplicity in model structure and assumptions. Our results highlight key considerations for the development and application of individual-based bioenergetic models in fisheries ecology, which can serve as a valuable and complementary tool to current methods in fisheries management.

## 1. Introduction

European pilchard (*Sardina pilchardus*) and European anchovy (*Engraulis encrasicolus*) are key components of global marine food webs, feeding mainly on zooplankton and serving as prey for higher trophic levels (Coll et al., 2007; Fanelli et al., 2023). Both species are heavily exploited by fisheries, resulting in approximately 60% of total landings in the Adriatic Sea and 30% of Mediterranean landings (average 2022–2023; FAO, 2025). Small pelagic fish dynamic is closely linked to environmental variability due to their plankton-based diet, short lifespan, and rapid turnover rates (Schwartzlose et al., 1999; Checkley Jr. et al., 2017), complicating their management (Fanelli et al., 2023). Moreover, in the last decade, a widespread pattern of reductions in size-at-age and size-at-puberty has been observed in many regional populations (Brosset et al., 2016; Chemello et al., 2023; Menu et al., 2023). These two life-history traits can impact fish population dynamics, as

---

* Corresponding author.
*E-mail address:* edonati@ogs.it (E. Donati).

https://doi.org/10.1016/j.ecoinf.2026.103736
Received 4 September 2025; Received in revised form 20 March 2026; Accepted 20 March 2026

fecundity scales with body weight (and thus body size; Marshall et al., 2022). Consequently, even relatively small reductions in size-at-age can lead to a dramatic decline in the population's reproductive potential (Barneche et al., 2018). Similarly, size at puberty determines the age at which individuals begin contributing to population renewal and the fishery recruitment size (Basilone et al., 2021; Johnson and Hixon, 2011): its decline may reflect physiological responses to environmental variability or adaptation to fishing pressure (Shin et al., 2005; Véron et al., 2020).

Fisheries have been under the spotlight as the main cause of the overexploitation status (Angelini et al., 2024; Čikeš Keč et al., 2024) and size decline of sardine and anchovy. However, changes in life-history traits, possibly driven by environmental pressures (Queirós et al., 2019; Verberk et al., 2021; Menu et al., 2023), may also have altered population structure and reduced abundance. Genetic and environmental impacts on growth, reproduction, and senescence shape an individual's fitness and life-history traits (Kooijman et al., 1989; Ricklefs and Wikelski, 2002) and ultimately population dynamics (Denney et al., 2002; Sæther et al., 2013). Thus, dynamically linking individual physiology and life-history traits to emergent population-level patterns is key to predicting population responses to environmental variability and anthropogenic stressors, and to informing their management.

Current knowledge of sardine and anchovy populations in the Adriatic Sea mainly derives from quantifying abundances at sea using direct methods (echosurveys, e.g., MEDIAS; Leonori et al., 2021), and indirect methods such as stock assessments (SAs). Environmental drivers (e.g. sea surface temperature, salinity, chlorophyll-a) can be explicitly incorporated into SAs to influence processes such as growth, recruitment and natural mortality (Punt et al., 2021): this can be done through functional relationships (Caserta et al., 2025) or by using covariates as an index of environmental influence (Crone et al., 2019), allowing the model to estimate how well they explain, for instance, annual recruitment deviations (Punt, 2023).

However, physiological and behavioural effects of environmental change on individuals, and ultimately on populations, are not mechanistically explored, and are limited to the range of observed environmental conditions (Kearney and Porter, 2009). Consequently, while SAs remain central to fisheries management, they may underrepresent the ecological complexity shaping population dynamics under environmental change and anthropogenic pressures. A mechanistic model that links individual physiology to environmental and anthropogenic drivers at fine temporal resolution, allowing population dynamics to emerge, would improve our ability to understand, predict, and manage these species under future scenarios (Rose et al., 2024).

The Dynamic Energy Budget (DEB) theory (Kooijman, 2010) provides a mechanistic framework to describe how individuals acquire and allocate energy to maintenance, growth, maturation, and reproduction throughout their life cycle. It focuses on individual biological processes as functions of environmental conditions, such as food availability and temperature (Jusup et al., 2017). DEB theory can be integrated into various modelling approaches to scale processes from individuals to populations or ecosystems (Thunell et al., 2023; van der Meer et al., 2022). One such approach is individual-based modelling (IBM), in which the population is modelled as a collection of specimens (Railsback and Grimm, 2011). When implemented within an IBM, DEB allows explicit representation of individual variability and the influence of environmental conditions on physiological performance enabling bottom-up scaling from individuals to populations (Martin et al., 2012; De Cubber, 2023). IBM frameworks also offer flexibility in representing biological rules and individual behaviour when quantitative data are lacking, allowing the use of qualitative information and general rules where appropriate (Nespeca et al., 2023). IBMs have been increasingly used to model fish population dynamics in DEB contexts (e.g.Brochier et al., 2018; Bueno-Pardo et al., 2020; Flores-Valiente et al., 2023) and offer potential for future scaling up to multiple species and for integrating the social and economic dimensions of fisheries within the same framework (Haase et al., 2023; Rose et al., 2015). Other IBMs have combined stock-assessment models with energy budgets to explore management scenarios, environmental effects, and the spatial distribution of European sea bass (*Dicentrarchus labrax*; Walker et al., 2020; Watson et al., 2022). More advanced bioenergetic IBMs, implemented in fully three-dimensional space, have also been developed for small pelagics, including sardine and anchovy (Gkanasos et al., 2021; Rose et al., 2015).

In this study, we develop a DEB-IBM model for European sardine and anchovy populations in the Adriatic Sea, SPelAgent (**S**mall **Pel**aging **Agent**). The aim is to provide an initial implementation of a new tool to study the ecology and population dynamics of small pelagic fish. We aim to investigate whether a relatively simple bioenergetic individual-based model, with fine temporal resolution, can reproduce realistic population dynamics and known biology of sardine and anchovy in the Adriatic Sea. The model, driven by daily temperature, food availability, and fishing, links individual physiology and variability to population dynamics, and could complement traditional approaches used for fisheries management. SPelAgent is implemented in the Julia Programming Language (Bezanson et al., 2017) for computational efficiency and flexibility. We first validate individual-level outputs by comparing simulated life-history traits with empirical data and known biology. At the population level, we assess model realism by comparing simulated biomass and catches with SAs, acoustic survey data, and fisheries statistics, which currently represent the only available reference for sardine and anchovy populations status. Finally, we outline the key challenges and solutions when scaling individual bioenergetic models to the population level. We identify the reasons behind inconsistencies between SPelAgent and observed data or SA. This framework provides a foundation for future eco-evolutionary studies on how environmental variability and fishery exploitation influence the life-history traits and population dynamics of sardine and anchovy in the Adriatic Sea.

## 2. Methods

### 2.1. Study species

Sardine and anchovy are serial batch spawners with indeterminate annual fecundity, yet they exhibit distinct ecological strategies shaped by environmental preferences and life-history traits (Morello and Arneri, 2009). Sardines spawn primarily during the colder months (October–May) in deeper offshore waters (60–120 m) and prefer colder, nutrient-rich conditions (9–16 °C; Regner et al., 1988). In contrast, anchovies spawn from April to October, with peaks in late spring and summer, favoring warmer, more productive coastal areas (Sinovčić and Zorica, 2006). Although both species are zooplanktivorous, sardines are able to filter feed phytoplankton (Garrido et al., 2007). Fecundity in both species is size-dependent, with anchovies releasing up to 20 batches and sardines 10–15 batches per spawning season (Sinovčić, 1986; Marano et al., 1998). Growth and survival of early life stages are tightly linked to temperature, salinity, and prey availability in both species (Regner, 1985), making recruitment highly sensitive to environmental fluctuations (Morello and Arneri, 2009). Sardines are more sensitive to warming and environmental variability due to narrower ecological tolerances, while anchovies are at greater risk from overfishing due to their tendency to form large schools, causing high catchability (Morello and Arneri, 2009). Species-specific fluctuations are historically attributed to a combination of fishing pressure and environmental drivers (Grbec et al., 2002).

### 2.2. SPelAgent

SPelAgent simulates fish bioenergetics, governed by Dynamic Energy Budget theory (Kooijman, 2010), and population processes (e.g. mortality and food competition), within an agent-based framework (Railsback and Grimm, 2011; see equations in Table 1). In ecological

**Table 1**

DEB model fluxes and equations used in SPelAgent. State variables dynamics and fluxes equations of the *abj* DEB model are shown in eqs. 1–10 and 18.

| Definition | Unit | Equation | Eq. number |
|---|---|---|---|
| Structure, $V$ | $cm^3$ | $\frac{dV}{dt} = \frac{\dot{p_G}}{[E_G]}$ | 1 |
| Reserve energy, $E$ | J | $\frac{dE}{dt} = \dot{p}_A - \dot{p}_C$ | 2 |
| Maturity, $E_H$ | J | $\frac{E_H}{dt} = \dot{p}_R, \quad E_H < E_H^p$ | 3 |
| Reproduction buffer energy, $E_R$ | J | $\frac{E_R}{dt} = \kappa_R \dot{p}_R$ | 4 |
| Assimilation | J $day^{-1}$ | $\dot{p}_A = \{\dot{p}_{Am}\} s_M f V^{2/3}$ | 5*,** |
| Mobilization | J $day^{-1}$ | $\dot{p}_C = E \frac{[E_G]\, \dot{\nu}\, s_M\, V^{2/3} + \dot{p}_S}{\kappa\, E + [E_G]\, V}$ | 6* |
| Somatic maintenance | J $day^{-1}$ | $\dot{p}_S = [\dot{p}_M] V$ | 7 |
| Growth | J $day^{-1}$ | $\dot{p}_G = \kappa\, \dot{p}_C - \dot{p}_S$ | 8 |
| Maturity maintenance | J $day^{-1}$ | $\dot{p}_J = \dot{k}_j\, E_H$ | 9 |
| Reproduction | J $day^{-1}$ | $\dot{p}_R = (1 - \kappa)\dot{p}_C - \dot{p}_j$ | 10 |
| Weight of 1 individual in SI | g | $W_W = W_V + W_E + W_R = w\left(d_V V + \frac{w_E}{\mu_E}\ (E + E_R)\right)$ | 11 |
| Temperature correction factor | | $T_c = e^{\frac{T_A}{T_R} - \frac{T_A}{T}}$ | 12 |
| Batch size (for 1 individual in the SI) | N | $N_{eggs} = F_b \cdot N(\mu, \sigma) \cdot (W_W - W_R); \mu = 0, \sigma = 50$ | 13 |
| Positive growth rate, r | $day^{-1}$ | $e \geq L/_{L_m}, r = T_c s_M \dot{\nu}\ \frac{\frac{e}{L} - \frac{1}{L_m}}{e + g}$ | 14*, *** |
| Thinning hazard | $day^{-1}$ | $h_t = \frac{2}{3}\ \frac{r}{c}; c_{sardine} = 5; c_{anchovy} = 15$ | 15 |
| Communal functional response | | $f_{comm} = \frac{X_{tot}\ \kappa_X}{\sum_i^N \left\{\dot{p}_{Am,i}\right\} {L_i}^2 s_{M,i} T_c \Delta t}$ | 16 |
| Deaths | N | $D_{tot} = D_{nat} + D_{catch} \sim Binomial\left(SI_{Nind}, 1 - e^{-\left(M_n + M_f\right)}\right)$ | 17 |
| Maximum length | cm | $L_m = f\, \kappa\, \frac{\{\dot{p}_{Am}\}}{[\dot{p}_M]} s_M$ | 18*,** |

Square brackets [] denote quantities expressed per unit of structural volume, whereas curly brackets {} indicate quantities per unit of structural surface area; a dot over a variable marks a flux (rate per time; e.g. energy flux, Kooijman, 2010).

Notation used here is described in the ODD protocol in the Supplementary Material.

[*] In the *abj* model, $s_M$ is equal to 1 before birth, and then increases with structural length until metamorphosis: $s_M = \max(1, \min(L, L_j)/L_b)$.

[**] $f$ is the standardised functional response of the standard DEB model. In our model $f$ is calculated as $f_{comm}$ in Eq. 16.

[***] where $e$ is the scaled reserve density, equal to $\frac{[E]}{[E_m]}$ and $L$ the structural length, equal to the physical length (cm) multiplied by the shape coefficient $\delta_M$.

applications, the terms *agent* and *individual* are often used interchangeably, as the modelled entity typically represents a biological individual (individual-based modelling; Railsback and Grimm, 2011). To ensure numerical efficiency while maintaining ecological realism, we use a superindividual approach (Parry and Bithell, 2012; Rose et al., 2015): a superindividual (SI) is a cohort of fish clones (the individuals) born on the same day (same age, length, life stage, etc.) and characterized by the same DEB parameter set (Table 2). With this approach, we avoid tracking billions of individuals in the simulations, as bioenergetic and population level (e.g. mortality) calculations are performed at the superindividual level. In this study, the term individual refers to each fish (biological entity) represented within a superindividual (the computational unit of the model).

The model is applied independently to the two species, anchovy and sardine, and runs at a daily time step. A schematic representation is shown in Fig.1, while a detailed description of SPelAgent is provided in Supplementary Material A, following the “Overview, Design concepts and Details” (ODD) protocol (Grimm, 2020).

### 2.2.1. *Julia framework and Agents.Jl*

Julia is a high-performance programming language designed for scientific computing, offering C-like speed and Python-like syntax (Bezanson et al., 2017). Key features include multiple dispatch, Just-In-Time (JIT) compilation, and parallel computing (Bezanson et al., 2017; Roesch et al., 2023). Julia addresses the “two-language problem” by combining readability and high-level performance in a single environment (Roesch et al., 2023).

Agents.jl (Datseris et al., 2024) is Julia's dedicated library for agent-based modelling of complex systems. Built-in tools simplify data collection, visualization, integration with other packages and offer superior speed and scalability than other programming frameworks (Datseris et al., 2024).

Agents.jl was chosen for developing SPelAgent due to its efficiency and adaptability in anticipation of future developments.

### 2.2.2. *Individual bioenergetics: Dynamic Energy Budget (DEB) theory in a nutshell*

Physiological processes of each individual are modelled using Dynamic Energy Budget (DEB) theory, a mechanistic framework that describes how an individual organism acquires and allocates energy in response to environmental conditions such as food concentration and temperature (Kooijman, 2010). Here we provide a brief introduction to DEB theory; extended documentation and examples of its applications can be found in van der Meer (2006); Kooijman (2010); Lika et al., (2011); Nisbet et al. (2012) and Jusup et al. (2017).

In DEB, an individual is characterized by four state variables – reserve ($E$, J), structure ($V$, $cm^3$), maturity ($E_H$, J) and reproduction buffer ($E_R$, J; see equation in Table 1) – whose dynamics are governed by energy fluxes (denoted as $\dot{p}$; Fig. 1). The reserve ($E$) is part of body mass and does not require energy for maintenance, but instead serves as the body's energy pool, which is mobilized to fuel all metabolic needs of the organism; the structure ($V$) represents the organism's physical part of the body requiring maintenance; maturity ($E_H$) is the cumulative energy invested into increasing organism's complexity and determines life-stage transitions from egg to juvenile (birth) and from juvenile to adult (puberty), requiring maintenance; reproduction buffer ($E_R$), represents the

**Table 2**

DEB parameters (estimated in DEBTool) and SPelAgent population parameters.

| Parameter | Sardine | Anchovy | Unit | Definition |
|---|---|---|---|---|
| $\{\dot{F}_m\}$ | 6.5 | 6.5 | $cm^2 day^{-1}$ | Maximum specific searching rate |
| $\{\dot{p}_{Am}\}$* | 554.351 | 11.1371 | $J\ cm^{-2}\ day^{-1}$ | Maximum specific assimilation coefficient |
| $\kappa_X$ | 0.8 | 0.8 | – | Digestion efficiency |
| $\dot{\nu}$* | 0.02165 | 0.01944 | $cm\ day^{-1}$ | Energy conductance rate |
| $\kappa$ | 0.883 | 0.9901 | – | Allocation fraction to soma |
| $\kappa_R$ | 0.95 | 0.95 | – | Reproduction efficiency |
| $[\dot{p}_M]$ | 438.602 | 54.67 | $J\ cm^{-3}\ day^{-1}$ | Somatic maintenance |
| $\dot{k}_j$ | 0.002 | 0.002 | $day^{-1}$ | Maturity maintenance rate |
| $[E_G]$ | 5017.55 | 5077.0 | $J\ cm^{-3}$ | Cost per unit of structure |
| $[E_m]$ | 25,605.127 | 572.8960 | $J\ cm^{-3}$ | Maximum reserve density $\frac{\{\dot{p}_{Am}\}}{\dot{\nu}}$ |
| $g$ | 0.2219 | 0.1139 | | Energy investment ratio $\frac{[E_G]}{\kappa\,[E_m]}$ |
| $E_H^b$ | 0.01578 | 0.00012 | J | Maturity at birth |
| $E_H^j$ | 0.18735 | 0.6741 | J | Maturity at metamorphosis |
| $E_H^p$ | 4553.63 | 244.0 | J | Maturity at puberty |
| $s_M$ | 2.25531 | 17.3829 | – | Acceleration factor |
| $E_0$ | 0.69402 | 0.01375 | J | Initial reserve of an egg |
| $\delta_M$ | 0.1152 | 0.1656 | – | Shape coefficient |
| $d_V$ | 0.2 | 0.2 | $g\ cm^{-3}$ | Specific density of structure (dry) |
| $\mu_E$ | 550,000.0 | 550,000.0 | $J\ mol^{-1}$ | Chemical potential of reserve |
| $\mu_V$ | 500,000.0 | 500,000.0 | $J\ mol^{-1}$ | Chemical potential of structure |
| $w_E$ | 23.9 | 23.9 | $g\ mol^{-1}$ | Molecular dry weight of reserve |
| $w_V$ | 23.9 | 23.9 | $g\ mol^{-1}$ | Molecular dry weight of structure |
| $w$ | 5 | 5 | – | Conversion factor from dry – to – wet weight |
| $L_b$ | 0.02794 | 0.01335 | – | Structural length at birth |
| $L_j$ | 0.06301 | 0.23201 | – | Structural length at metamorphosis |
| $L_p$ | 1.19937 | 1.50 | – | Structural length at puberty |
| $L_m$* | 2.23 | 3.47 | – | Structural maximum length |
| $T_A$ | 8000 | 9800 | Kelvin | Arrhenius species specific temperature |
| $T_R$ | 293 | 293 | Kelvin | Reference temperature |
| *repro_start* | 270 | 90 | day | Starting day of reproductive period |
| *repro_end* | 90 | 270 | day | Ending day of reproductive period |
| $F_b$ | 400 | 450 | $eggs\ batch^{-1}\ g^{-1}$ | Relative batch fecundity (free gonad weight) |
| $M_0$ | 1.08 | 1.06 | $y^{-1}$ | Natural mortality age class 0+ |
| $M_1$ | 0.86 | 1.01 | $y^{-1}$ | Natural mortality age class 1+ |
| $M_2$ | 0.69 | 0.82 | $y^{-1}$ | Natural mortality age class 2+ |
| $M_3$ | 0.62 | 0.69 | $y^{-1}$ | Natural mortality age class 3+ |
| $M_4$ | 0.48 | 0.62 | $y^{-1}$ | Natural mortality age class 4 + |

Notation used here is described in the ODD protocol in the Supplementary Material.

* $\{\dot{p}_{Am}\}$ and $\dot{\nu}$ values are shown here prior to being multiplied by $s_M$ (*abj* model), while $L_m$ value already accounts for it: $s_M$ is equal to 1 before birth, and then increases with structural length until metamorphosis: $s_M = \max(1, \min(L, L_j)/L_b)$.

energy invested in the development of gonads tissues and gametes.

Reserves increase with energy assimilated from ingested food ($\dot{p}_X$, Fig. 1), through the assimilation flux ($\dot{p}_A$), which is proportional to the surface area of structure (Kooijman, 2010). The mobilization of energy stored from the reserve $E$ follows the $\kappa$-rule: a fraction ($\kappa$) of this mobilized energy is allocated to the somatic branch, to first cover somatic maintenance ($\dot{p}_S$) proportional to volume of structure, and growth ($\dot{p}_G$) of structure V; the remaining fraction ($1-\kappa$) is directed to the maturity/reproduction branch, which includes maturity maintenance ($\dot{p}_J$) proportional to maturity, and maturation/reproduction ($\dot{p}_R$), which increases the maturity up to puberty, and is afterwards used to build gonads and gametes. The $\kappa$ -rule ensures a consistent energy partitioning strategy throughout the life cycle, preventing direct competition between growth and reproduction (Kooijman, 2010). Under energy-limited conditions, energy stored in the reproduction buffer can be reallocated to support somatic maintenance. Dynamics of state variables and equations for energy fluxes are presented in Table 1.

Reserve, structure and reproduction buffer (in adults) determine the size and the weight of the individual, while maturity has no physical volume. The weight of the organism is calculated as the sum of the weight of the structure ($W_V$), the reserve ($W_E$) and the reproduction buffer ($W_R$), if present, as shown in Eq. 11 in Table 1 (Haberle et al., 2023; Nisbet et al., 2012). Each egg inherits an initial amount of energy, based on the reserve density of the mother at egg formation (Haberle et al., 2023), which is then used by the embryo for its development.

In the standard DEB model (Kooijman, 2020), organisms are assumed to be isomorphic, meaning that shape remains constant as size increases, and surface area scales with $V^{2/3}$. However, many species – including sardines and anchovies – exhibit a phase of metabolic acceleration between birth and puberty, during which surface scales linearly with V, and growth is faster than predicted by isomorphy. We therefore used the "*abj*" variant of the DEB standard model which accounts for this phenomenon (Kooijman et al., 2011).

In DEB theory, all physiological rates are affected by temperature through the correction factor $T_c$, calculated from the Van't Hoff–Arrhenius equation (van der Meer, 2006; Eq. 12 in Table 1). The higher $T_{A,}$ the more sensitive the species is to temperature variation (Lika et al., 2011).

### 2.2.3. Parameterisation

The DEB parameters for both anchovy and sardine were initially obtained from the Add-my-Pet (AmP) database (Marques et al., 2018; https://www.bio.vu.nl/thb/deb/deblab/add_my_pet/, accessed in August 2024). As part of the preliminary analysis, the model was run with the initial parameter sets, under observed long-term climatological conditions (see Section 2.3). These runs tested the model's ability, given

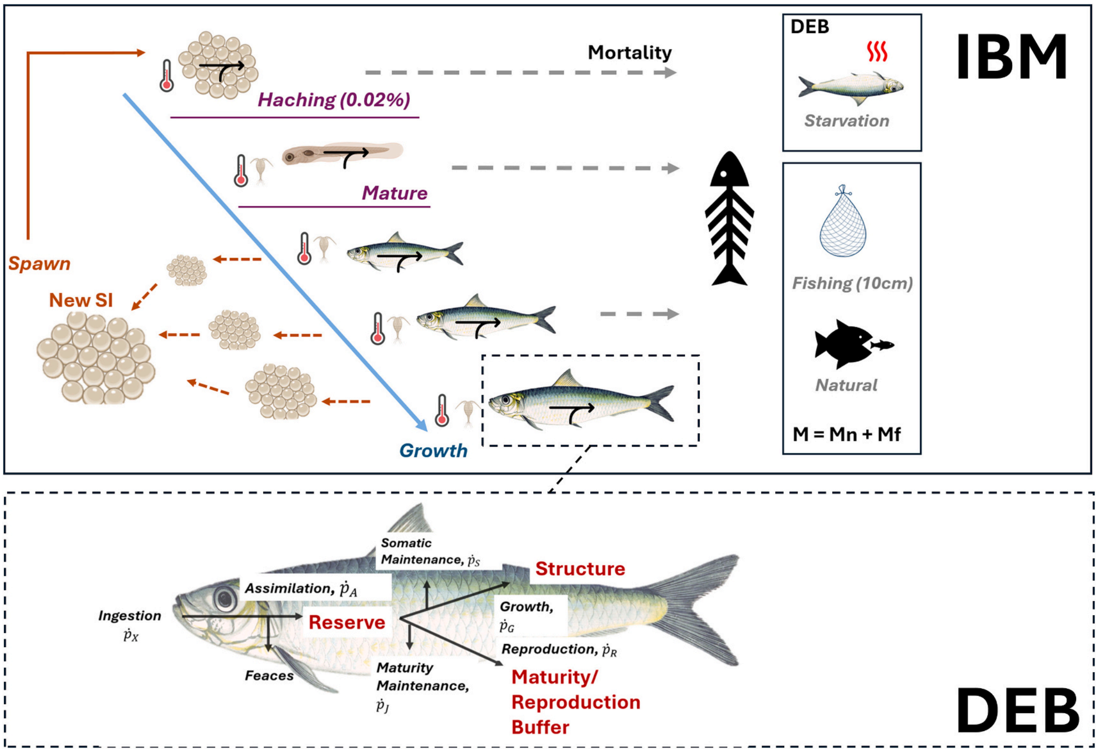

**Fig. 1.** Schematic representation of SPelAgent model. Top: the IBM simulates spawning, mortality and density-dependent access to food. Individual physiology is modelled according to the Dynamic Energy Budget Theory (DEB) and forced by food and temperature: embryos do not eat, while juveniles and adults feed on zooplankton. DEB theory governs growth and life-stages transition. State variables: Reserve ($E$), Structure ($V$), Maturity ($E_H$) and Reproduction ($E_R$; adults only). Energy fluxes are denoted as $\dot{p}$.

the parameterisation, to realistically reproduce key life-history traits, including lifespan, gonado-somatic index (GSI), reproduction rates, and age and size at puberty.

The results for anchovy (Pecquerie and Kooijman, 2015; MRE:0.256; completeness 2.6) produced realistic outputs and the AmP parameter set was therefore deemed appropriate for use in the subsequent DEB-IBM simulations (Table 2).

In contrast, using the AmP DEB parameter set for sardine (Nunes et al., 2025; MRE: 0.065; completeness 2.5) resulted in underestimated reproductive output, with individuals producing approximately only two batches per year — well below the expected 10–15 batches (Morello and Arneri, 2009). A new parameter set was estimated using the standard AmP fitting procedure in DEBtool (DEBtool., 2024; Marques et al., 2018) and empirical data from the Adriatic and Mediterranean Sea (Basilone et al., 2023; Dulčić, 1994; Mustać et al., 2020). To minimise the risk of inconsistencies across datasets, zero-variate life-history information (scalar values at specific life stages) for Adriatic Sea populations was obtained from the literature (Morello and Arneri, 2009). These data included age and length at birth and puberty, expected lifespan, and relative fecundity. We calculated weight at stage transitions from the correspondent length-at-stage records (specific to the Adriatic Sea) using FishBase (Froese and Pauly, 2025). Uni-variate data (vectors of dependent variables) included length-at-age observations (cm at year of age) from individuals sampled in the Adriatic Sea (Mustać et al., 2020), along with length–weight data (Mustać et al., 2020) and larval growth measurements (mm at day of age; Dulčić, 1994). We also included length-at-age data from other Mediterranean Sea populations (Basilone et al., 2023), as these values were consistent with the ranges reported for the Adriatic Sea.

This revised set (MRE = 0.209, completeness 2.6; Table 2) improved SPelAgent performance for sardines – increasing the average reproductive output approximately to eight batches per year, better matching the expected reproductive rates while maintaining realistic growth predictions. The estimated parameter set was used for further DEB-IBM simulations.

The species-specific DEB parameter sets were assigned to all identical fish clones comprising the SI. Among SIs of the same species, minor variation in some biological traits and parameters was implemented to reflect natural variability (see the ODD protocol in Supplementary Material A).

### 2.2.4. *Population (IBM)*

Population dynamics in the model emerge from individual bioenergetics, which determine growth, development, and reproduction, computed at the superindividual level. The resulting fish size influences reproductive success, while maturation governs recruitment and the onset of reproduction in the population.

SIs perform different processes according to the life-stage of their individuals: egg SIs use stored energy for growth and maturation until they hatch into juveniles. A fixed embryo mortality proportion of 99.98% is applied once just before hatching to reflect early-life stage mortality (Haberle et al., 2023). Juveniles and adults feed from the environment, with access to food regulated by density dependence through a communal functional response (Haberle et al., 2023). Juveniles and adults are subject to natural mortality (representing ageing and predation), and to fishing mortality if the size of the fish in the SI exceeds 10 cm.

2.2.4.1. *Spawning.* Spawning occurs during the species-specific reproductive seasons whenever a SI of adult fish has sufficient energy in its reproduction buffer to produce a viable batch. The batch size is determined by the individual free-gonad weight ($W_W$ - $W_R$) and species-specific relative batch fecundity ($F_b$). The batch fecundity is set at 400 eggs per batch per gram of free-gonad weight for sardines and 450 for anchovies (Casavola et al., 1996a, 1996b). The batch fecundity ($F_b$) is scattered by a white noise (see Eq. 13 in Table 1) to simulate natural fluctuations in reproductive output. All eggs produced on the same day by different adult SIs are aggregated into a single new egg SI. Since both species are multiple-batch spawners and reproduce several times within a season, this approach ensures computational efficiency and prevents an excessive increase in the number of SIs in the simulation.

*2.2.4.2. Density dependence.* Food assimilation is density-dependent regulated through the communal functional response *($f_{comm}$, Haberle et al., 2023),* that is the ratio (bounded to 1) between the total assimilable food in the water basin and the ideal food requirements of all individuals in the SIs in the population, in the given timestep (one day; see Eq. 16 in Table 1):

$$f_{comm} = \frac{X_{tot}\,\kappa_X}{\sum_i^N \{\dot{p}_{Am,i}\} L_i^{\,2} s_{M,i} T_c\,\Delta t}$$

The numerator is the total zooplankton ($X_{tot}$) in the water basin, expressed in Joules and estimated from biogeochemical reanalysis (see Section 2.3), multiplied by the assimilation efficiency $\kappa_X$. The denominator is the maximum assimilation of the population, calculated as the product of the individual surface-area-specific maximum assimilation rate $\{\dot{p}_{Am}\}$, the individual acceleration factor $s_M$ (*abj* model; Kooijman, 2020), the square of structural length $L^2$ (corresponding to $V^{2/3}$), and the temperature correction factor $T_c$. This formulation indicates the capacity of the system to sustain the population, given the available food: if the food available is equal to the requested food, $f_{comm}$ is equal to 1 and individual assimilation will be at its maximum; if food is less, $f_{comm}$ will decrease, limiting growth capacity and, if too low, leading to starvation (Kooijman, 2010).

*2.2.4.3. Mortality.* In SPelAgent, mortality arises from three sources: starvation, natural mortality (ageing and predation), and fishing mortality. Starvation mortality occurs when an individual can no longer meet maintenance costs by mobilising energy from the reserve and the reproduction buffer (Kooijman, 2010). Due to the superindividual approach, this means that all individuals comprising the SI – all being identical clones and experiencing identical environmental conditions – die of starvation. Consequently, for this mortality type, the entire SI is removed from the simulation.

Natural and fishing mortality, meanwhile, affect the individuals within the SI. Natural mortality (here representing senescence and predation) is modelled as a fixed age-dependent daily probability of death ($M_n$), while fishing mortality ($M_f$) affects only fish longer than 10 cm, regardless of their life stage. The sum of $M_n$ and $M_f$ defines the daily total instantaneous mortality (*M*; Hilborn and Walters, 1992). The number of deaths each time step is stochastically sampled using a binomial distribution from the number of individuals (Nind*)* in the SI (Eq. 17 in Table 1). Resulting deaths are partitioned into natural and fishing components using the relative contribution of each mortality rate ($M_n$ and $M_f$ respectively) to the total instantaneous mortality rate *M* (Baranov catch-equation; Hilborn and Walters, 1992; for more details see the ODD protocol in the Supplementary Material). A sensitivity analysis of the model responses to varying fishing mortality, at both individual and population levels, is provided in Supplementary Material B.

The number of surviving individuals (Nind) in each SI decreases with deaths (D) over time. When Nind falls below a fixed fraction of its initial value ($Nind_o$), the SI is flagged as dead and removed from the active population. This fraction is calculated at model initialisation based on natural mortality rates, ensuring a realistic lifespan of the SI under the effect of natural mortality alone.

In populations with individuals of different life stages and sizes, competing for food, DEB theory results in unrealistic energetic advantage for juveniles due to their favorable surface-to-volume ratio (i.e., high assimilation capacity relative to maintenance needs; Kooijman, 2024). The resulting population dynamic is dominated by juvenile recruitment, which outcompetes adults, ultimately causing adults to die of starvation (juvenile-driven cycle; Kooijman, 2024). To prevent this unrealistic model behaviour, a thinning hazard is applied to juveniles, and added to the total instantaneous mortality rate *M* (Kooijman, 2024). The thinning hazard ($h_t$) is calculated according to the formulation provided in the DEBtool package (DEBtool., 2024; *popDyn* folder; *abj* model): it is proportional to the growth rate *r* and modulated to avoid population collapse through the coefficient $2/3\,c$ (Eq. 14 and 15 in Table 1). Since SPelAgent does not allow shrinking (reabsorption of structure when starving; Kooijman, 2010), the thinning hazard is applied only when the growth rate is positive, which is calculated from the scaled reserve *e*, structural length *L*, acceleration factor $s_M$, maximum structural length $L_m$, and energy investment into growth *g* (Eq. 14 in Table 1). To further increase realism and avoid juvenile-driven cycles, individual variability in somatic maintenance cost and in energy at puberty is represented by randomly sampling $[\dot{p}_M]$ and $E_H^p$ of each SI from a normal distribution centred on the nominal value (Table 2) with a standard deviation of 0.1.

### 2.3. Environmental data

Water temperature data were obtained from Copernicus Marine Service (doi:10.25423/CMCC/MEDSEA_MULTIYEAR_PHY_006_004_E3R1) where physical reanalysis data are available at 1/24° horizontal resolution, for the period from 1987 to 2023, covering the entire Mediterranean Sea (Escudier et al., 2021).

Zooplankton reanalysis data were obtained from the 3D Biogeochemical Flux Model (BFM; Vichi et al., 2023) upon request through the CMEMS platform (1999–2023; 1/24° resolution; Cossarini et al., 2021). BFM includes four zooplankton functional types (Vichi et al., 2023). We computed total zooplankton availability by summing the integrated carbon concentrations over the water column, of all zooplankton groups, across all grid cells of the Adriatic Sea. The resulting zooplankton biomass, expressed as milligrams of carbon (mgC), was converted to joules assuming that 1 g of carbon corresponds to 46 kJ (Postel et al., 2000; Salonen et al., 1976).

For the climatological simulations, daily averages of temperature and total zooplankton concentration were calculated from the reanalysis time series (Fig. 2A).

### 2.4. Stock assessments

SPelAgent is designed to apply daily natural and fishing mortality to SIs to determine the number of deaths from each cause. Age-specific natural and fishing mortality rates ($y^{-1}$) were derived from SAs, converted to daily values (by dividing by 365 days, 1 year of simulation) and entered as daily $M_n$ and $M_f$, respectively. Both mortality rates were used as initial proxies for the real total mortality probability (*M*) in SPelAgent, which was then used to calculate the daily number of deaths in the SIs (Eq. 17, Table 1). SPelAgent performance in long-term simulations was evaluated against SA data for small pelagics in the Adriatic Sea (Geographical Sub-Areas, GSAs, 17 and 18 of the General Fisheries Commission for the Mediterranean, GFCM; Angelini et al., 2019a;b); comparing simulated population biomass and catches with SA estimates (Total Stock Biomass; TSB) and reported catches. Given that SAs are the only large-scale evaluation of stocks status, together with echosurvey, our comparison positioned SPelAgent performance relative to them, assessing the DEB-IBM's realism in long-term hindcast runs rather than attempting formal validation.

Data from SAs conducted in 2018 (SA2018; Angelini et al., 2019a, 2019b) and 2024 (SA2024; stock assessment forms not yet available) were used to cover the longest simulation period, i.e.; years 1975–2024 (assessment id SA2018: STAR_ANE_2018_1718 and STAR_PIL_2018_1718; assessment id SA2024: STAR_ANE_2024_1718 and STAR_PIL_2024_1718; available at: https://www.fao.org/gfcm/data/star/en/).

From SA2018 and Libralato et al. (2020), we used age-specific

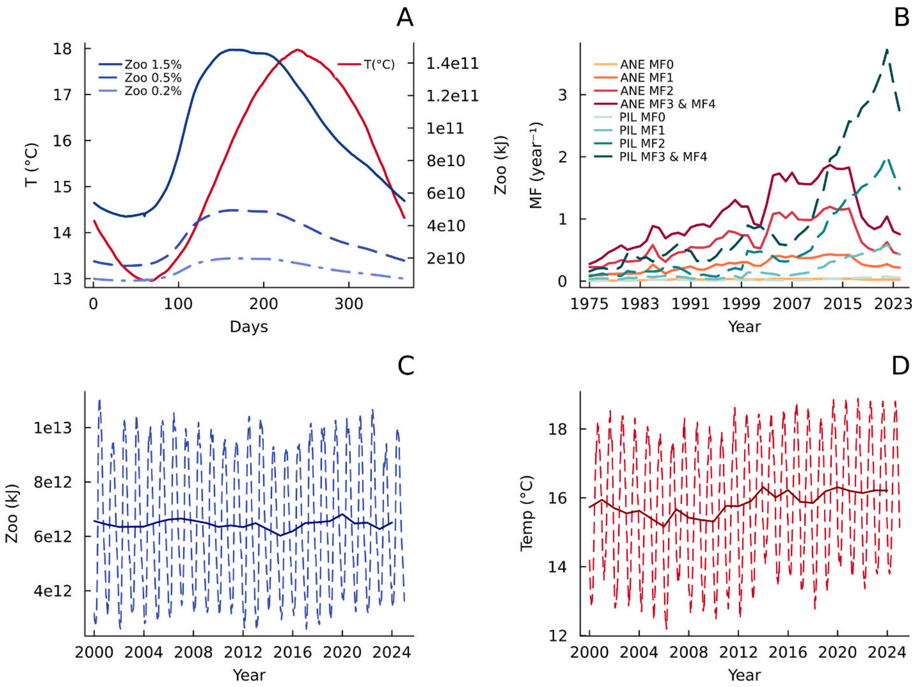

**Fig. 2.** Environmental and fishing mortality inputs in SPelAgent. A) Climatological temperature and total zooplankton, integrated over the 0–200 m water column in the Adriatic Sea derived from Copernicus Marine Service. The different fractions of total zooplankton used to tune sardine and anchovy populations are shown (1.5%; 0.5% and 0.2%). B) Time series of fishing mortality rates from SA2018 and SA2024. C) Daily total zooplankton in the Adriatic Sea for 2000–2024, expressed in kJ. D) Daily water temperature in the Adriatic Sea (0–200 m depth) for 2000–2024, expressed in °C, with solid line representing the annual averages trend.

natural and fishing mortality ($F_a$), TSB and Spawning Stock Biomass (SSB) estimates for 1975–2000, for both sardine and anchovy (Fig. 2B; catch at age stock assessment; FLSAM; Kell et al., 2007; Aeberhard et al., 2018). For the period 2000–2024, the latest SA (SA2024) provided only fishing mortality across selected age classes ($F_{bar}$), for both species. Therefore, to reconstruct age-specific fishing mortality ($F_a$), $F_{bar}$ values were scaled using the $F_a/F_{bar}$ proportions estimated from the SA2018 for the period 2000–2018. Moreover, SA2024 provided only TSB estimates for sardine, as it is stochastic surplus-production model in continuous time (SPiCT; Pedersen and Berg, 2017); consequently, a reference for the SSB was not available. For anchovy, SA2024 showed a sharp increase in fishing mortality at age 1 (F1) — up to four times higher than previous estimates — due to an update in the fish age-assignment methodology (Caserta et al., 2025). These values caused unrealistic population crashes in SPelAgent simulations. To prevent this, SA2024 age-specific fishing mortalities were rescaled to match the 2018 estimates for anchovy, applying a correction based on the difference between 1999 (from SA2018) and 2000 (from SA2024), thus obtaining a meaningful time series of fishing mortalities (Fig. 2B). Natural mortality from SA2018 was used as a reference for 2000–2024 for both species, since SA2024 did not report natural mortality for sardine and latest estimates for anchovy were not sustainable in SPelAgent, similarly to fishing mortality.

### 2.5. Long term simulations

The model was run separately for each species using climatological conditions as set-up simulations driven by daily average temperature (°C) and zooplankton biomass (mgC $m^{-2}$) in the upper 200 m of water column, for the period 1987–2024 (see Section 2.3). Climatological simulations were initialised with 1000 egg SIs (each representing 10 million eggs) and run for 50 years to reach a dynamic steady state. The fraction of accessible daily zooplankton biomass was tuned to obtain a total fish biomass consistent with SA estimates (SA2024). Results were used to assess emergent population structure, individual traits, and model validity against published data and literature benchmarks.

Hindcast simulations (1975–2024) were initialised with the steady-state population structure obtained from the set-up climatological runs. Additionally, we included a 10-year spin-up under climatological forcing (see Section 2.3) to ensure stable dynamics. After the spin-up period, the hindcast simulations were driven by age-specific fishing mortality rates derived from SA results (SA2024; see Section 2.4). We used daily values of temperature and integrated zooplankton biomass (mgC $m^{-2}$) in the upper 200 m of water column, from the temporal time series of the Adriatic Sea (1987–2023). Temperature was used to calculate daily values of the temperature correction factor $T_c$ according to Eq. 12 (Table 1), which influences all metabolic fluxes (see Section 2.2.2); zooplankton biomass, once converted to joules (see Section 2.3), entered the communal functional response eq. (Eq.16; Table 1). To cover the full hindcast period (1975–2024), missing environmental forcing for years at the start and the end of the time series were filled using daily averages from the two nearest available years (Fig. 2C and D).

## 3. Results

### 3.1. Corroboration

Under climatological conditions, SPelAgent simulations produced a dynamically stable population structure (Fig. 3 S1 and A1): 73% of sardines and 83% of anchovies belong to age 0+ class, while more than 50% of the biomass is concentrated in age classes 1+ and 2+. The modelled lifespan aligns with observed data for sardine, with individuals reaching up to 8+ years (vs. 9 years reported by Morello and Arneri, 2009). Almost 1% of individuals are over 5+ years old. For anchovy, the modelled lifespan is slightly underestimated: the maximum reported age is 4 years with less than 1% of individuals surviving beyond age 3+, compared to the reported maximum age of 6 years (Morello and Arneri, 2009).

After puberty, sardines took more than 1 month to release a batch (median: 44 days; Q1 = 34; Q3 = 67 days). Adults released up to 13

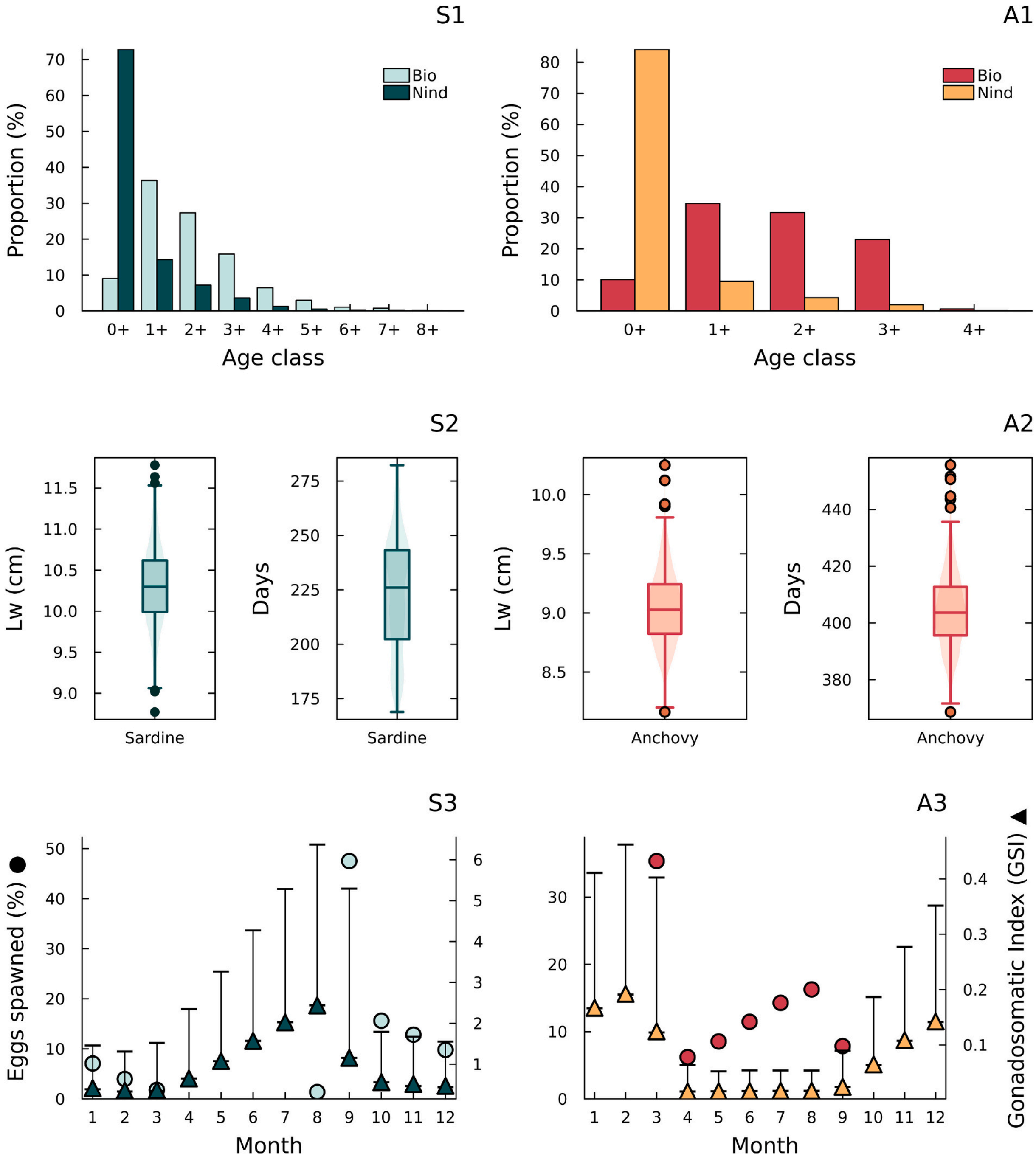

**Fig. 3.** Results of individual life-history of climatological simulations. Sardine and anchovy are colour-coded in green and orange, respectively. From top to bottom: yearly average percentage of number of individuals (Nind) and biomass (Bio) distributed across age classes (S1 and A1); boxplots showing median and quantiles of size and age at puberty (S2 and A2); monthly seasonal variation in mean GSI values (▲) and percentage of batches released relative to the total batches in one reproductive season (●) (S3 and A3). (For interpretation of the references to colour in this figure legend, the reader is referred to the web version of this article.)

batches during the reproductive season (median = 7; Q1 = 5; Q3 = 8), with a median interval of 25 days between batches (Q1 = 8; Q3 = 31). The updated parameterisation, combined with thinning hazards and variability in $E_H^p$ and $[\dot{p}_M]$, reduced reproductive synchronisation and prevented excessive resource depletion during recruitment, resulting in more realistic adult growth and reproduction. Simulation of anchovy reproduction was also consistent with expected outputs: anchovies mature at the onset of the reproductive season and are immediately ready to release eggs, with a median of 20 batches per season (Q1 = 11; Q3 = 22), and a median interval of 10 days between batch releases (median; Q1 = 3; Q3 = 14).

Median size at puberty (Fig. 3 S2 and A2; L50) is estimated at 10.3 cm (Q1 = 9.99 cm; Q3 = 10.6 cm) for sardine and around 9 cm (Q1 = 8.8 cm; Q3 = 9.2 cm) for anchovy. Age at puberty (Fig. 3 S2 and A2) slightly deviates from recent SAs, particularly for anchovy. While historical sources suggest both species reach maturity by the end of their first year, SPelAgent estimates that 50% of sardines mature by the age of 224 days (median; Q1 = 201 days; Q3 = 244 days), whereas more than 50% of anchovies require over one year to mature (median = 402 days; Q1 = 395 days; Q3 = 411 days). Reproductive timing (Fig. 3 S3 and A3)

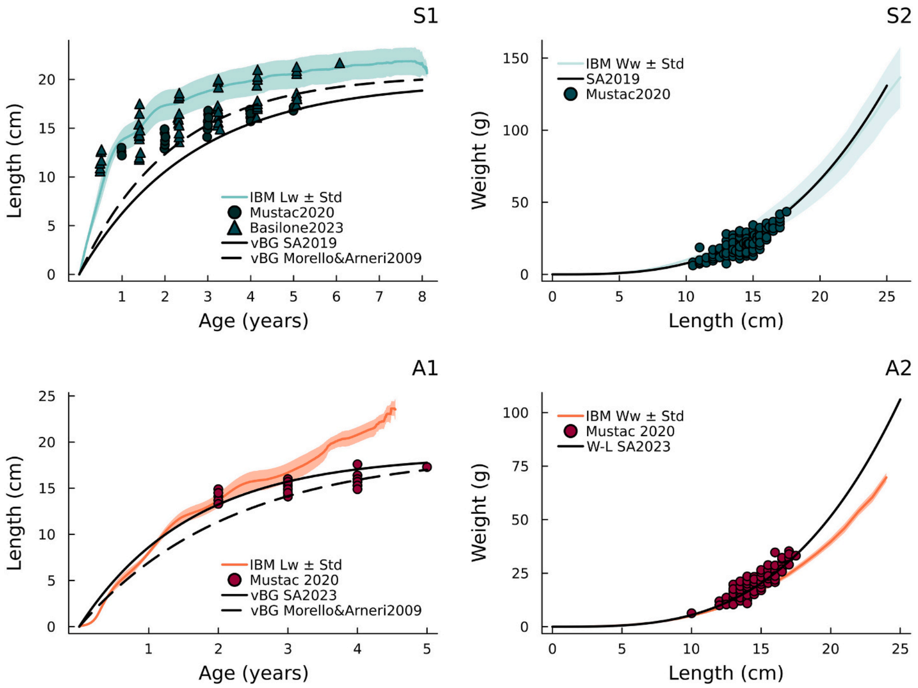

**Fig. 4.** Length and weight curves of sardine and anchovy in SPelAgent. Length-at-age (left) and allometric length–weight (right) relationships for sardine (top: S1; S2) and anchovy (bottom: A1; A2). Observed data are shown as scattered points: triangles in S1 represent Basilone et al. (2023), while dots in all plots represent Mustać et al. (2020). In S1 and A1, the continuous black line indicates the von Bertalanffy growth model from Morello and Arneri (2009), and the dashed line the most recent growth model reported in stock assessment reports (SA2019; Čikeš Keč et al., 2021; SA2023; Angelini et al., 2024). In S2 and A2, the continuous black line represents the latest stock-assessment-based allometric length–weight relationship.

for both species showed a pronounced peak at the onset of the spawning season — September for sardines and March for anchovies — followed by a smaller secondary peak in August for anchovies. This pattern reflects the accumulation of energy into the gonads during the non-reproductive season, as indicated by the inverse seasonal trend between gonadosomatic index (GSI) and egg release. The allometric length–weight relationship is well reproduced (Fig. 4 S2 and A2), consistent with data from Mustać et al. (2020) and in agreement with equations reported in recent SAs. However, length-at-age tends to be overestimated across the full lifespan of sardine and especially for older anchovy individuals (Fig. 4 S1 and A1).

### 3.2. *Stock assessment comparison*

To match total stock biomass (TSB) estimates from SAs, the accessible fraction of the total zooplankton biomass was set to 0.5% for sardine and 1.5% for anchovy. This relatively small percentage reflects that zooplankton is also consumed by other predators, and that not all prey biomass is simultaneously available to the sardine and anchovy populations. Notably, reproducing catch levels for anchovy required only 0.2% of zooplankton biomass to be accessible.

Sardine hindcast simulations reproduced the stable TSB observed from 2000 to 2010 (Fig. 5 S1), followed by a marked decline, consistent with the rising $F_{bar}$ and the subsequent collapse in reported catches. However, initial catch values were overestimated (60000 t vs. 20000–30000 t reported by GFCM for 2000–2008; Fig. 5 S3). After 2011, the model captured observed catch trends both qualitatively and quantitatively.

SPelAgent struggled to replicate anchovy TSB trends — showing a decline between 2000 and 2005, whereas SAs reported an increase followed by a stable phase (Fig. 5 A1). In later years, the SPelAgent model showed a partial recovery of TSB, consistent with stabilised $F_{bar}$, though it did not capture the sharp drop observed between 2010 and 2012. Reduced food input improved the catch estimates, reproducing general trends and variability, though fluctuations were dampened compared to assessment outputs (Fig. 5 A3).

Neither SPelAgent nor SAs reproduce magnitude, temporal trend or the high interannual variability observed in fishery-independent MEDIAS echosurvey (Fig. 5 S2 and A2).

## 4. Discussion

SPelAgent is an individual-based model for sardine and anchovy populations in the Adriatic Sea. The model successfully links individual physiology with environmental variability, allowing changes in key life-history traits to emerge and influence population demography, while maintaining simple structure and assumptions.

### 4.1. *Consistency with known ecophysiology*

In SPelAgent, individual traits emerge from bioenergetic processes and population-level dynamics such as competition, recruitment, and mortality. The model reproduced plausible individual lifespan and population structure, both in abundance and biomass across age classes (Fig. 3; S1 and A1). Most life-history patterns were consistent with the literature (Fig. 3 and Fig. 4).

The average physical length at puberty for sardine (10.3 cm) and anchovy (9 cm) falls within the reported ranges (8-12 cm for sardine; 7-10 cm for anchovy; Morello and Arneri, 2009). For anchovy, more recent assessments report L50 around 7–8 cm (Angelini et al., 2024), suggesting earlier reproduction compared to historical observations, as noted by Brosset et al. (2016) for other regions of the Mediterranean Sea. In SPelAgent, 50% of anchovies mature at about 402 days of age, consistent with the recent assessments (age-0+ immature; Angelini et al., 2024), while 50% of sardines mature at 224 days, consistent with historical data.

Reproductive seasonality matched the known biology: anchovy spawned at the start of the season with a characteristic double peak in

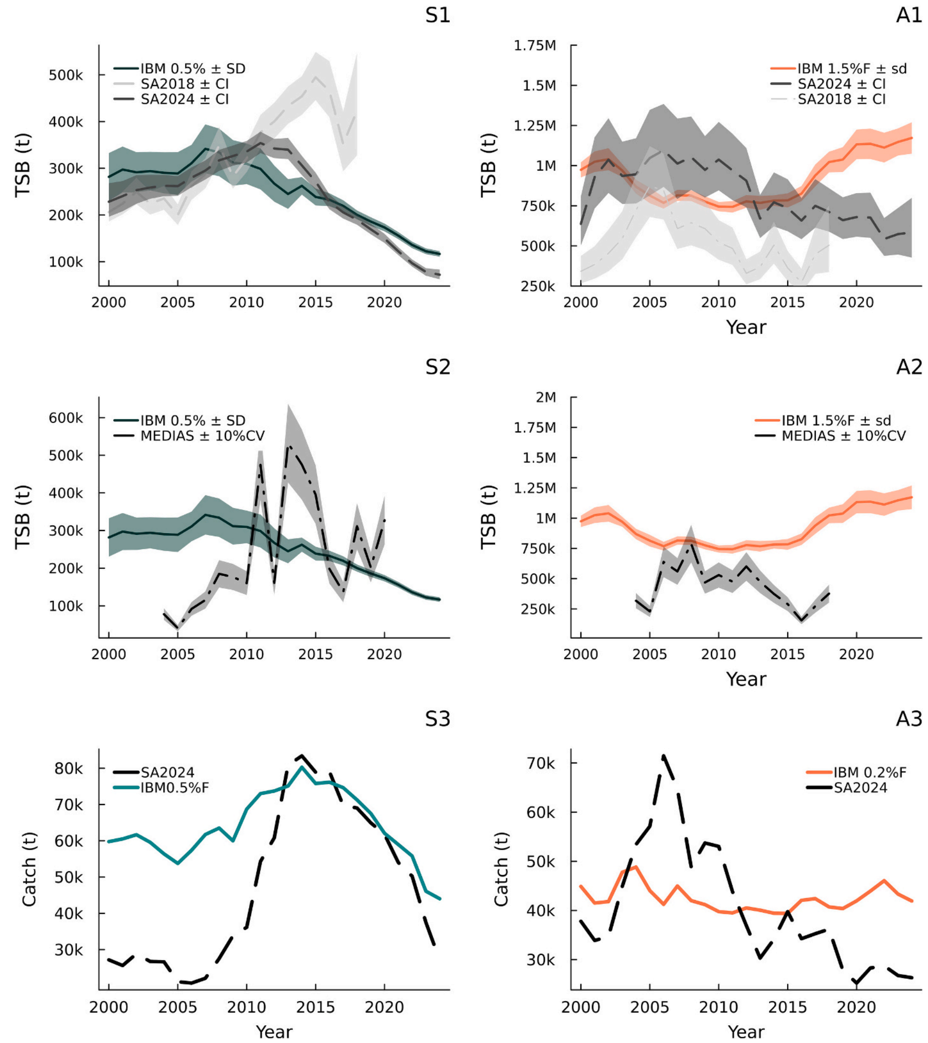

**Fig. 5.** Results of hindcast simulations of total stock biomass (TSB) and catches for sardine (left, green; "S" panels) and anchovy (right, orange; "A" panels) for the period 2000–2024 (solid line), compared with stock assessment estimates SA2024 and SA2018, or MEDIAS echo survey. S1 and A1: temporal trends of TSB compared with SA2024 (dashed black line) and SA2018 (grey dot-dashed line); S2 and A2: temporal trends of TSB compared with MEDIAS echosurvey (black dot-dashed line) assuming uncertainty equal to 10% of the coefficient of variation CV; S3 and A3: comparison between estimated and observed catches. (For interpretation of the references to colour in this figure legend; the reader is referred to the web version of this article.)

egg release, while sardine spawning was mostly synchronised in September, without a secondary peak (Fig. 3; last row). Anchovy spawn during spring–summer, when elevated temperatures and greater food availability increase assimilation rates and, consequently, the allocation of energy to reproduction (income breeder; Palomera et al., 2007; Somarakis et al., 2004; Brosset et al., 2016). In contrast, sardines spawn during winter (Morello and Arneri, 2009), relying on stored reserves (high maximum reserve density [$E_m$]; capital breeder strategy; Ganias et al., 2007; Pethybridge et al., 2014; Brosset et al., 2016). However reproduction under oligotrophic conditions intensified competition with juveniles (juvenile-driven cycles; Kooijman, 2024). Moreover, sardines mature rapidly (~240 days), so most one-year-olds join the spawning population at the start of the next reproductive season (single peak). Anchovies mature in ~400 days, with juveniles joining the spawning population the following year, but later than already mature adults (secondary peak).

Despite the simple reproduction mechanism in SPelAgent, reproductive rates and frequency were realistically captured, but greater realism in seasonal energy allocation is desirable. In SPelAgent, spawning occurs when, during the reproductive season, an adult has enough energy in the gonads to release a batch of the given fecundity. This approach causes energy to accumulate in the gonads during the non-reproductive period (high gonadosomatic index; GSI; Fig. 3 S3 and A3), which is the opposite of field observations (Basilone et al., 2021; Brosset et al., 2016; Chemello et al., 2023; Đurović et al., 2018). Pecquerie et al. (2009) extended the standard DEB model with a batch preparation module specific for multiple-batch spawners. This approach will be the next extension in SPelAgent: the gonadosomatic index (GSI) could be calculated from the energy stored in the batch preparation pool, consistently with the seasonal release of eggs.

Growth patterns in length and weight were satisfactory (Fig. 4), despite length-at-age predictions being slighlty overestimated for both species, in different ways. For sardine, predictions were consistent with observations from the Alboran Sea (Basilone et al., 2023), which were – at all ages – higher than other (Adriatic) observations and SA models (Fig. 4; S1) (Mustać et al., 2020; Morello and Arneri, 2009; and SA2024). For anchovy, size is realistic in younger age classes but overestimated in older individuals (Fig. 4; A1): the emergent maximum length matches the value reported in FishBase (25 cm), but is well above Adriatic observations (18 cm; Morello and Arneri, 2009). The high estimated $L_m$ and acceleration factor $s_M$ for anchovy (Table 2) likely result from a very high allocation fraction to soma ($\kappa = 0.9901$) in the current parameterisation, which attempts to capture the rapid growth of eggs and juveniles. Accounting for the vertical segregation of early life stages, compared to adults, during the parametrization routine and in the IBM, could improve parameterisation and model realism. In the Mediterranean, eggs and larvae typically inhabit the upper 20–50 m (Coombs et al., 2004; Zorica et al., 2019), where warmer temperatures may largely be responsible of early growth acceleration (Brochier et al., 2018; Menu et al., 2023; Rose et al., 2015).

In the AmP database, entries for both species have a relatively low level of completeness (2.5 out of a maximum 10), which is typical for long-lived species where most available data are not collected in DEB-specific surveys or laboratory experiments, which are challenging and costly (Cheng et al., 2025; Lika et al., 2011). This is why often data from the literature is used. Such datasets provide a general metabolic characterisation of the species but are often insufficient to capture region-specific conditions of sub-populations (van der Meer, 2006; Kooijman et al., 2008; Cheng et al., 2025). The new parameterisation of sardines relied primarily on literature for the Adriatic Sea (Dulčić, 1994; Mustać et al., 2020), supplemented — after confirming their ecological consistency — by a smaller set of observations from other Mediterranean regions (Basilone et al., 2023). The new parameters improved model realism and likely reflects acclimatisation to region-specific environmental conditions, rather than local adaptation, which should be confirmed by genetic analyses. Current parameterisation of both species would benefit from additional field surveys designed for DEB purposes (individual length and age estimation through otoliths, GSI) and detailed environmental information for each area-dataset (e.g. seasonality and depth gradients). Additional basin-specific datasets would mitigate the model's tendency to overestimate length, especially its bias toward growth patterns typical of the Alboran Sea (Basilone et al., 2023).

### 4.2. Challenges in scaling from individuals to population

When scaling from individuals to populations, several artefacts emerged: the high influx of juveniles due to their synchronisation in puberty and reproduction (juvenile-driven cycle; Kooijman, 2024) led to severe resource depletion and excessive starvation mortality among older SIs, whose higher somatic maintenance made them more vulnerable. The unrealistic synchronisation of recruitment also required applying a higher egg mortality at hatching (99.98%) than the 99.8% proposed by Haberle et al. (2023). This parameter was highly sensitive: even small deviations (e.g.; 99.95%) amplified juvenile-driven cycles — especially in sardine — causing adult starvation and delayed maturation, while higher values (e.g., 99.99%) delayed the attainment of steady state. A more realistic solution would involve the extended batch preparation module of Pecquerie et al. (2009), where egg production emerges from energy fluxes and body condition rather than fixed fecundity. The percentage mortality could also be made dependent on egg reserve density inherited from the mother's energetic state at spawning, so that egg condition would influence the probability of hatching.

Sardines proved particularly sensitive to juvenile-driven cycles, but the adopted strategies – thinning hazard and variability in DEB parameters – partially mitigated negative effects on adult survival and reproduction. However, the thinning hazard is a pragmatic solution to correct unrealistic model behaviour: the hazard mimics the strong intraspecific competition for food during early life stages which cannot emerge directly from the bioenergetic framework. Increasing biological realism would provide a more consistent solution. For example, introducing life-stage-specific food types would reduce competition and prevent unrealistic adult starvation (Kooijman, 2024), with juveniles feeding mainly on small zooplankton and adults switching among prey types, including larger zooplankton that is inaccessible to early larvae (Borme et al., 2009, 2013). Additional improvements could include size-dependent predation mortality and spatial heterogeneity, which would partially segregate juveniles and adults and reduce competition, particularly during the spawning season (Kooijman, 2024).

The communal functional response did not mitigate the strong intraspecific competition, as it assumes uniform food access regardless of size or competitive ability (Haberle et al., 2023). While useful for estimating carrying capacity under given environmental conditions, the current formulation requires revision as it is less suited to capturing realistic feeding dynamics and size-based competition.

One way to better account for density dependence is to modify the denominator of the scaled functional response by adding a density-dependence term (DeAngelis et al., 1975; Menu, 2024). While conceptually sound, this approach requires calibrating additional parameters (Menu, 2024), which is difficult without a gold-standard reference of population stock time series. An alternative approach from ecotoxicology modelling would scale the functional response by a stress factor (Jager et al., 2023) to reflect food competition.

However, the most biologically realistic option is to explicitly model resource dynamics by linking it to the oceanographic condition (Rose et al., 2010). Although technically challenging, this would directly couple the system's biogeochemistry — which shapes plankton structure and productivity — to higher trophic levels. Such integration is widely seen as the ultimate goal for bioenergetic individual-based models, and several frameworks are moving in this direction (Brochier et al., 2018; Gkanasos et al., 2021; Politikos et al., 2015; Rose et al., 2015). Although promising, such approach was premature at this stage, as the priority was to establish a simple and robust model reference for future developments.

### 4.3. Integrating stock assessment and environmental reanalysis for population reconstruction

In SPelAgent, sardine and anchovy required together at most 2% of the total daily zooplankton biomass. This low exploited fraction reflects that zooplankton is consumed by other predators and that only part of its biomass is accessible to sardine and anchovy. Moreover, according to published ecosystem models, meso- and micro-zooplankton have a turnover rate of 30–40 year$^{-1}$ (production over biomass, P/B; Coll et al., 2007; Libralato et al., 2010), corresponding to a daily production rate of 10.95% of their biomass. Thus, the ratio between small pelagics' daily consumption of zooplankton biomass in SPelAgent (2% d$^{-1}$) and the reported zooplankton daily turnover (10.95% d$^{-1}$) indicates that sardine and anchovy together exploit approximately 18.3% of the daily zooplankton production, which agrees with estimates from recent ecosystem models (Libralato et al., 2020).

#### 4.3.1. Comparing population composition between SPelAgent and stock assessments

SPelAgent and SAs produced different population structures and biomass trends for anchovy in hindcast simulations, mainly due to differences in recruitment dynamics arising from the need to control juvenile-driven cycles in SPelAgent. Such discrepancies can occur when comparing approaches based on different modelling paradigms, namely a bioenergetic mechanistic model versus a statistical framework, like SAs.

When reproducing total stock biomass (TSB) and catches (Fig. 5; hindcast simulations), model performance was satisfactory for sardines, requiring 0.5% of total zooplankton biomass. For anchovies, however, different food levels were required to match either TSB (requiring 1.5% of total zooplankton biomass) or catches (requiring 0.2% of total zooplankton biomass).

For anchovy, SA models estimate a high proportion of juveniles compared to adults ($TSB >> SSB$; Supplementary Material C). Contrary to SAs, SPelAgent hindcast results show that the anchovy population biomass consists mostly of adults ($TSB \approx SSB$; see Fig. SC.1 in Supplementary Material C), which also largely represent the catchable population (size at puberty close to the imposed fishery recruitment size of 10 cm; Fig. 3.A2). The higher exploitation rates reported in SA2024 (Angelini et al., 2024) could not be used to reduce the catchable population biomass (≈ SSB) as they were not sustainable in SPelAgent, especially for young individuals (see Section 2.4). Therefore, we tuned SPelAgent to either match the catches by lowering the food level (which reduces TSB, SSB and, consequently, the size of the catchable population), or the SA-estimate of TSB, by increasing the food level.

The different population structure (TSB/SSB proportions) for anchovy indicates that the biomass and/or number of recruits (juveniles) differs between the two models. This discrepancy is unlikely to result from the representation of reproductive traits in SPelAgent: the model reproduced the length–weight relationship, fecundity (input based on literature), and onset of puberty realistically (Section 4.1). In addition, the fishery recruitment size is set at 10 cm (see Section 2.2.4), which is above stock assessment estimates, meaning that immature individuals are unlikely to be harvested.

Therefore, the TSB/SSB mismatch could result from: (i) differences in estimating the proportion of old and large individuals contributing to recruitment; (ii) difficulties in modelling early larval growth in the acceleration phase while keeping adult growth realistic; (iii) excessive mortality of juveniles; or (iv) the combination of these factors. The first point likely reflects juvenile-driven cycles and the therefore the difficulty of sustaining adult survival (see Section 4.2). The second point could be mitigated through improved SPelAgent parameterisation and by considering the spatial segregation of eggs and early-larvae (see Section 4.1). To avoid overly suppressing anchovy recruitment (iii), an attempt to relax the high egg-mortality rate from 99.98% to 99.95% didn't reduce the gap between TSB and SSB, and had instead reintroduced the characteristic juvenile-cycle asynchrony (see Section 4.1). We therefore believe that most of the discrepancy between the two models arises from the need to control for juvenile-driven cycles by limiting the influx of juveniles, through both thinning hazards and high egg mortality. The reduced number of juveniles likely explain why SPelAgent could not sustain the higher exploitation rates estimated by SA2024 in the first place. Increasing model realism (Section 4.2), could enable SPelAgent to support a larger proportion of immature individuals, and enhance our understanding of the recruitment variability.

SPelAgent already accounts for some factors known to influence recruitment success: the effects of temperature, food availability and intraspecific competition for resources on fish growth and fertility, as well as the influence of maternal status at spawning on egg condition (Fernández-Corredor et al., 2021; Green, 2008; Houde, 2016). A future spatially explicit version of SPelAgent could further resolve recruitment by tracking how exposure to different environmental conditions influences individual vital rates, and ultimately population dynamics, enhancing its relevance for management.

#### 4.3.2. *Implications when transferring fishing mortality across frameworks*

Differences between SPelAgent and SAs in population structures, model assumptions, and sources and timing of mortality can result in varying stock dynamics when SA-derived fishing mortality is applied in an IBM.

SPelAgent was designed from the outset to apply a daily probability of death from total mortality, incorporating both natural and fishing components (Haberle et al., 2023). Within the DEB framework, endogenous process-based mortality is limited to ageing, easily included in natural mortality, and starvation (Kooijman, 2010), included in SPelAgent to simulate food supply stress on individual physiology. Aging and starvation are not directly modelled in SAs. In DEB-IBM models, any source of mortality beyond ageing and starvation must be introduced as an external process, for which the modeller must choose an appropriate functional form — for example, a fixed percentage (as for hatching mortality in our case), a rate, or a probability.

The most straightforward estimates of natural and fishing mortalities come from SA models, and were therefore initially used in SPelAgent as a proxy of death probability due to natural causes and fishery. However, SAs estimate annual age-specific fishing mortality for a cohort (or population) of fish. SPelAgent applies mortality daily to a fraction of the population, a superindividual (millions of fish clones), by dividing annual natural and fishing mortality rates by the standard year length (365 days). This downscaling from annual age-class rates to daily superindividual mortality rates is a reasonable approximation for an initial model implementation. Still, in SA models, the fishing mortality F is co-estimated with biomass, and tuned to the internal assumptions of the assessment (Hilborn and Walters, 1992).

Furthermore, assessment estimates often differ over time due to varying assumptions and methodologies based on data availability (Cadrin, 2025). This occurred for anchovy, where the increase in age-0 and age-1 fishing mortalities between SA2018 and SA2024 (change in individual age assignment; Caserta et al., 2025) caused population collapse in SPelAgent (TSB–SSB mismatch; Section 4.3.1).

The need to reduce the fishing mortality (Section 2.4) introduced a new inconsistency, as shown by the sensitivity analysis (Supplementary Material B): within SPelAgent, productivity is maximised at $F = 2$ for both sardine and anchovy (Fig. SB.1 A7 and SB.2 S7). For sardine, the fishing mortality time series derived from SA approaches $F \approx 4$ (Fig. 2.B; green), indicating overexploitation consistent with assessment results (Angelini et al., 2019b). For anchovy, the applied (adjusted) fishing mortality never exceeds $F = 2$ (Fig. 2B; orange). Consequently, in SPelAgent, the anchovy population is not overexploited, contrary to SA estimates from 2000 onward (Angelini et al., 2024). After the 2012 effort reduction (Fig. 5A1), SPelAgent shows a rapid population rebound without major change in catches (Fig. 5A3; solid orange line) whereas reported catches decline (Fig. 5A3; dashed black line; SA2024). The overall stability of zooplankton and temperature time series over the same period (Fig. 2C–D) suggests that this pattern reflects fishery underexploitation: reduced fishing mortality further relaxes fishing constraints, allowing the population to increase enough to offset the reduced catches.

In future model refinements, fishing mortality should be modelled using approaches independent of SAs. One option is to directly remove observed catches that correspond to the estimated number of individuals extracted from the population, based on length-based selectivity and catch data (Menu, 2024). However, this approach requires subjective assumptions on the seasonal distribution of fishing effort and catches, to prevent over-depletion and negative population biomass.

The most comprehensive approach would be to model fishing pressure by including the social and operational aspects of the fishery, calibrating catchability to specific harvesting methods, and fleet behaviour, effort, and profitability (Fulton et al., 2011; Marchal et al., 2013; Rose et al., 2015). This requires detailed spatial and temporal effort data and follows the approach used in ecosystem models such as Ecospace (Ecopath with Ecosim software; EwE; Pauly et al., 2000) and other End-to-End models (Rose et al., 2015). Although such data are difficult to obtain comprehensively, this method could enable SPelAgent to fully exploit the strength of IBM by explicitly linking ecological processes with the social dimensions of fishing and management (Burgess et al., 2020; Haase et al., 2023; Lindkvist et al., 2020). In this scenario, fishing mortality would no longer be considered as an external input to the model, but rather a result of the system dynamics (Fulton et al., 2011; Marchal et al., 2013).

## 5. Conclusions

This study introduces SPelAgent: a bioenergetic mechanistic individual-based model for sardine and anchovy populations in the Adriatic Sea, developed in Julia. We assessed whether the model reproduces the biology and population dynamics of small pelagic species and, if not, identified the mechanisms responsible for any discrepancies.

The model reproduced key life-history patterns and realistic trends in biomass and catches. By linking environment effects on individual fish physiology up to population dynamics, SPelAgent can provide valuable insights to complement traditional management tools. The mechanistic formulation of SPelAgent enables hypothesis testing in case of inconsistency with empirical data or different modelling frameworks. For instance, minor simplifications in growth, reproduction, and competition generated artefacts such as synchronised recruitment, limiting quantitative agreement with stock assessments (SAs). Exploring the trade-off in food levels required to match either SA biomass or catches revealed that controlling for juvenile-driven cycles reduced recruitment compared to SA. Therefore, SPelAgent resulted in a different population structure for anchovy and applying the stock assessment fishing mortality produced inconsistent biomass and catches trajectories.

We recommend to explicitly represent fishery exploitation within individual-based models, leveraging their flexibility to incorporate processes such as fleet behaviour, fishing effort, and catchability. We also highlighting the need for improved representations of feeding, prey dynamics and spatial processes in individual-based frameworks, to avoid unrealistic population behaviour.

## CRediT authorship contribution statement

**E. Donati:** Writing – review & editing, Writing – original draft, Visualization, Validation, Software, Methodology, Investigation, Formal analysis, Data curation, Conceptualization. **N. Marn:** Writing – review & editing, Validation, Supervision, Methodology, Investigation, Conceptualization. **I. Haberle:** Writing – review & editing, Validation, Supervision, Methodology, Investigation, Data curation, Conceptualization. **S. Libralato:** Writing – review & editing, Validation, Supervision, Resources, Project administration, Methodology, Investigation, Conceptualization.

## Funding

ED was supported by the Ministry of University and Research (Italy) and University of Trieste PhD scholarship. The scholarship was co-funded by the Department of Life Sciences (DSV; University of Trieste, Italy) and the National Institute of Oceanography and Applied Geophysics (OGS; Italy). This work was partially funded by the project FAIRSEA (Fisheries in the Adriatic Region – a Shared Ecosystem Approach) funded by the 2014–2020 Interreg V-A Italy – Croatia CBC Programme [Standard project ID 10046951] and by the project NECCTON (New Copernicus Capability for Trophic Ocean Networks) funded by Horizon Europe RIA under grant agreement n∘101081273.

NM and IH were funded by the Croatian Science Foundation grant IP-2022-10-5901 (QPlast).

This research did not receive any other grants from funding agencies in the public; commercial; or not-for-profit sectors.

## Declaration of competing interest

The authors declare that they have no known competing financial interests or personal relationships that could have appeared to influence the work reported in this paper.

## Acknowledgements

We would like to thank the curators of the Add-My-Pet project and teachers of the 9th Edition of the Dynamic Energy Budget School for valuable comments and suggestions on model parameterisation and development. We thank Diego Borme, Silvia Angelini, Stefano Piani, Stefano Campanella, Fabio Giordano and Alberto Ghedin for their valuable insights on the ecology of the species and technical support.

We thank Reviewer 1, Reviewer 3, Reviewer 4, and especially Reviewer 2, for their valuable comments, constructive suggestions, and the additional insights they brought to the interpretation of our results.

## Appendix. Supplementary data

Supplementary data to this article can be found online at https://doi.org/10.1016/j.ecoinf.2026.103736.

## Data availability

An illustrative version of SPelAgent is available at https://github.com/elisadonati23/SPelAgent_v0

## References

Aeberhard, W.H., Flemming, J.M., Nielsen, A., 2018. Review of state-space models for fisheries science. Annu. Rev. Stat. Appl. 5, 215–235. https://doi.org/10.1146/annurev-statistics-031017-100427.

Angelini, S., Arneri, E., Belardinelli, A., Biagiotti, I., Bratina, P., Brunel, T., Canduci, G., Cacciamani, R., Calì, F., Colella, S., Costantini, I., Croci, C., De Felice, A., Domenichetti, F., Donato, F., Gašparević, D., Hintzen, N., Ibaibarraga, L., Juretic, T., Kule, M., 2019a. Stock Assessment Form: Anchovy (*Engraulis encrasicolus*) in GSA 17–18 (Adriatic Sea; Italy; Croatia; Slovenia; Albania; Montenegro); Referencer Year 2018; Reporting Year 2019. General Fisheries Commission for the Mediterranean (GFCM); FAO.

Angelini, S., Arneri, E., Belardinelli, A., Biagiotti, I., Bratina, P., Brunel, T., Canduci, G., Cacciamani, R., Calì, F., Colella, S., Costantini, I., Croci, C., De Felice, A., Domenichetti, F., Donato, F., Gašparević, D., Hintzen, N., Ibaibarraga, L., Juretic, T., Kule, M., 2019b. Stock Assessment Form: Sardine (European Pilchard) in GSA 17–18 (Adriatic Sea; Italy; Croatia; Slovenia; Albania; Montenegro); Referencer Year 2018; Reporting Year 2019. General Fisheries Commission for the Mediterranean (GFCM); FAO.

Angelini, S., Biagiotti, I., Bratina, P., Čikeš Keč, V., Costantini, I., De Felice, A., Donato, F., Gašparević, D., Juretic, T., Kule, M., Leonori, I., Modic, T., Palluqi, A., Pesic, A., Santojanni, A., 2024. Stock Assessment Form (SAF): European Anchovy (*Engraulis encrasicolus*) in GSAs 17 and 18 (Adriatic Sea); Reference Year 2023; Reporting Year 2024. General fisheries Commission for the Mediterranean (GFCM); FAO.

Barneche, D.R., Robertson, D.R., White, C.R., Marshall, D.J., 2018. Fish reproductive-energy output increases disproportionately with body size. Science 360 (6389), 642–645. https://doi.org/10.1126/science.aao6868.

Basilone, G., Ferreri, R., Aronica, S., Mazzola, S., Bonanno, A., Gargano, A., Pulizzi, M., Fontana, I., Giacalone, G., Calandrino, P., Genovese, S., Barra, M., 2021. Reproduction and sexual maturity of European sardine (*Sardina pilchardus*) in the Central Mediterranean Sea. Front. Mar. Sci. 8, 715846. https://doi.org/10.3389/fmars.2021.715846.

Basilone, G., Ferreri, R., Bonanno, A., Genovese, S., Barra, M., Aronica, S., 2023. Age and growth of European sardine (*Sardina pilchardus*) in the Central Mediterranean Sea: implications for stock assessment. Fishes 8 (4), 202. https://doi.org/10.3390/fishes8040202.

Bezanson, J., Edelman, A., Karpinski, S., Shah, V.B., 2017. Julia: a fresh approach to numerical computing. SIAM Rev. 59 (1), 65–98. https://doi.org/10.1137/141000671.

Borme, D., Tirelli, V., Brandt, S.B., Fonda Umani, S., Arneri, E., 2009. Diet of *Engraulis encrasicolus* in the northern Adriatic Sea (Mediterranean): ontogenetic changes and feeding selectivity. Mar. Ecol. Prog. Ser. 392, 193–209. https://doi.org/10.3354/meps08214.

Borme, D., Tirelli, V., Palomera, I., 2013. Feeding habits of European pilchard late larvae in a nursery area in the Adriatic Sea. J. Sea Res. 78, 8–17. https://doi.org/10.1016/j.seares.2012.12.010.

Brochier, T., Auger, P.A., Pecquerie, L., Machu, E., Capet, X., Thiaw, M., Mbaye, B.C., Braham, C.B., Ettahiri, O., Charouki, N., Sène, O.N., Werner, F., Brehmer, P., 2018. Complex small pelagic fish population patterns arising from individual behavioral responses to their environment. Prog. Oceanogr. 164, 12–27. https://doi.org/10.1016/j.pocean.2018.03.011.

Brosset, P., Lloret, J., Muñoz, M., Fauvel, C., Van Beveren, E., Marques, V., Fromentin, J.M., Ménard, F., Saraux, C., 2016. Body reserves mediate trade-offs between life-history traits: new insights from small pelagic fish reproduction. R. Soc. Open Sci. 3 (10), 160202. https://doi.org/10.1098/rsos.160202.

Bueno-Pardo, J., Petitgas, P., Kay, S., Huret, M., 2020. Integration of bioenergetics in an individual-based model to hindcast anchovy dynamics in the Bay of Biscay. ICES J. Mar. Sci. 77 (2), 655–667. https://doi.org/10.1093/icesjms/fsz239.

Burgess, M.G., Carrella, E., Drexler, M., Axtell, R.L., Bailey, R.M., Watson, J.R., Cabral, R.B., Clemence, M., Costello, C., Dorsett, C., Gaines, S.D., Klein, E.S., Koralus, P., Leonard, G., Levin, S.A., Little, L.R., Lynham, J., Madsen, J.K., Merkl, A., Wilcox, S., 2020. Opportunities for agent-based modelling in human dimensions of fisheries. Fish Fish. 21 (3), 570–587. https://doi.org/10.1111/faf.12447.

Cadrin, S.X., 2025. Misinterpreting retrospective patterns in fishery stock assessment. ICES J. Mar. Sci. 82 (2). https://doi.org/10.1093/icesjms/fsaf014.

Casavola, N., Rizzi, E., Marano, G., 1996a. First data on batch fecundity and relative fecundity of *Sardina pilchardus* (Walbaum; 1792) (Clupeidae) in the South-Western Adriatic Sea. Bol. Inst. Esp. Oceanogr. 12, 53–63.

Casavola, N., Marano, G., Rizzi, E., 1996b. Batch fecundity of *Engraulis encrasicolus* L. in the South-Western Adriatic Sea. Sci. Mar. 60 (2–3), 369–377.

Caserta, V., Punt, A.E., Arneri, E., Berginc, T., Keč, V.Č., Costantini, I., De Felice, A., Donato, F., Leonori, I., Santojanni, A., Angelini, S., 2025. Incorporating key environmental drivers in European anchovy (Engraulis encrasicolus) stock assessment model in the Adriatic Sea. ICES J. Mar. Sci. 82 (9), fsaf171. https://doi.org/10.1093/icesjms/fsaf171.

Checkley Jr., D.M., Asch, R.G., Rykaczewski, R.R., 2017. Climate; anchovy; and sardine. Ann. Rev. Mar. Sci. 9, 469–493. https://doi.org/10.1146/annurev-marine-122414-033819.

Chemello, G., Cerrone, G.L., Tavolazzi, V., Donato, F., Tiralongo, F., Gioacchini, G., 2023. One year study on the reproductive biology; ovary characterization and age of the European sardine (*Sardina pilchardus*) in the middle-West Adriatic Sea. Front. Mar. Sci. 10, 1266894. https://doi.org/10.3389/fmars.2023.1266894.

Cheng, M.C.F., Geček, S., Marn, N., Giacoletti, A., Sarà, G., King, N., Ragg, N.L.C., 2025. From lab to ocean: leveraging targeted experiments for advancements in mussel aquaculture through mechanistic modelling. Aquaculture 594, 741434. https://doi.org/10.1016/j.aquaculture.2024.741434.

Čikeš Keč, V., Angelini, S., Arneri, E., Belardinelli, A., Biagiotti, I., Boscolo Palo, G., Bratina, P., Brunel, T., Canduci, G., Cacciamani, R., Calì, F., Colella, S., Costantini, I., De Felice, A., Domenichetti, F., Donato, F., Gašparević, D., Hintzen, N., Ibaibarraga, L., Juretic, T., Ticina, V., 2021. Stock assessment form (SAF): sardine (*Sardina pilchardus*) in GSAs 17 and 18 (Adriatic Sea); reference year 2019; reporting year 2021. General Fisheries Commission for the Mediterranean (GFCM); FAO.

Čikeš Keč, V., Angelini, S., Biagiotti, I., Bratina, P., De Felice, A., Juretić, T., Kule, M., Leonori, I., Pešić, A., Santojanni, A., Giannoulaki, M., Ramirez, J.G., 2024. Stock Assessment Form: *Sardina pilchardus* in GSAs 17–18 (Reference Year 2023). General Fisheries Commission for the Mediterranean (GFCM).

Coll, M., Santojanni, A., Palomera, I., Tudela, S., Arneri, E., 2007. An ecological model of the northern and Central Adriatic Sea: analysis of ecosystem structure and fishing impacts. J. Mar. Syst. 67, 119–154. https://doi.org/10.1016/j.jmarsys.2006.10.002.

Coombs, S.H., Boyra, G., Rueda, L.D., Uriarte, A., Santos, M., Conway, D.V.P., Halliday, N.C., 2004. Buoyancy measurements and vertical distribution of eggs of sardine (*Sardina pilchardus*) and anchovy (*Engraulis encrasicolus*). Mar. Biol. 145 (5), 959–970. https://doi.org/10.1007/s00227-004-1389-4.

Cossarini, G., Feudale, L., Teruzzi, A., Bolzon, G., Coidessa, G., Solidoro, C., Amadio, C., Lazzari, P., Brosich, A., Di Biagio, V., Salon, S., 2021. High-resolution reanalysis of the Mediterranean Sea biogeochemistry (1999–2019). Front. Mar. Sci. 8, 741486. https://doi.org/10.3389/fmars.2021.741486.

Crone, P.R., Maunder, M.N., Lee, H., Piner, K.R., 2019. Good practices for including environmental data to inform spawner–recruit dynamics in integrated stock assessments: small pelagic species case study. Fish. Res. 217, 122–132. https://doi.org/10.1016/j.fishres.2018.12.026.

Datseris, G., Vahdati, A.R., DuBois, T.C., 2024. Agents.Jl: a performant and feature-full agent-based modeling software of minimal code complexity. Simulation 100 (10), 1019–1031. https://doi.org/10.1177/00375497211068820.

De Cubber, L., 2023. Unravelling mechanisms behind population dynamics; biological traits and latitudinal distribution in two benthic ecosystem engineers: a modelling approach. Prog. Oceanogr. 212, 103112. https://doi.org/10.1016/j.pocean.2023.103112.

DeAngelis, D.L., Goldstein, R.A., O'Neill, V., 1975. A model for tropic interaction. Ecology 56 (4), 881–892. https://doi.org/10.2307/1936298.

DEBtool. 2024. DEBtool [Software Package] (Version 2024/01/25). Kooijman; S. A. L. M.; Marques; G.; Augustine; S.; Lika; D.; & Marn; N. https://github.com/add-my-pet/DEBtool_M.

Denney, N.H., Jennings, S., Reynolds, J.D., 2002. Life-history correlates of maximum population growth rates in marine fishes. Proc. R. Soc. B Biol. Sci. 269, 2229–2237. https://doi.org/10.1098/rspb.2002.2138.

Dulčić, J., 1994. Estimation of age and growth of sardine; *Sardina pilchardus* (Walbaum; 1792); larvae by reading daily otolith increments. Fish. Res. 22, 265–277. https://doi.org/10.1016/0165-7836(94)90004-3.

Đurović, M., Joksimović, A., Pešić, A., Marković, O., Regner, S., Mandić, M., Ikica, Z., 2018. Reproductive pattern of the anchovy; *Engraulis encrasicolus* (Linnaeus; 1758); in the Boka Kotorska Bay (Montenegro; southern Adriatic Sea). Acta Adriat. 59 (2), 173–184. https://doi.org/10.32582/aa.59.2.2.

Escudier, R., Clementi, E., Cipollone, A., Pistoia, J., Drudi, M., Grandi, A., Lyubartsev, V., Lecci, R., Aydogdu, A., Delrosso, D., Omar, M., Masina, S., Coppini, G., Pinardi, N., 2021. A high-resolution reanalysis for the Mediterranean Sea. Front. Earth Sci. 9, 702285. https://doi.org/10.3389/feart.2021.702285.

Fanelli, E., Da Ros, Z., Menicucci, S., Malavolti, S., Biagiotti, I., Canduci, G., De Felice, A., Leonori, I., 2023. The pelagic food web of the Western Adriatic Sea: a focus on the role of small pelagics. Sci. Rep. 13, 14554. https://doi.org/10.1038/s41598-023-40665-w.

FAO, 2025. The State of Mediterranean and Black Sea Fisheries 2025, Special edition. Gen. Fish. Comm. Mediterr, Rome. https://doi.org/10.4060/cd7701en.

Fernández-Corredor, E., Albo-Puigserver, M., Pennino, M.G., Bellido, J.M., Coll, M., 2021. Influence of environmental factors on different life stages of European anchovy (*Engraulis encrasicolus*) and European sardine (*Sardina pilchardus*) from the Mediterranean Sea: a literature review. Reg. Stud. Mar. Sci. 41, 101606. https://doi.org/10.1016/j.rsma.2020.101606.

Flores-Valiente, J., Lett, C., Colas, F., Pecquerie, L., Aguirre-Velarde, A., Rioual, F., Tam, J., Bertrand, A., Ayón, P., Sall, S., Barrier, N., Brochier, T., 2023. Influence of combined temperature and food availability on Peruvian anchovy (*Engraulis ringens*) early life stages in the northern Humboldt current system: a modelling approach. Prog. Oceanogr. 215, 103034. https://doi.org/10.1016/j.pocean.2023.103034.

Froese, R., Pauly, D., 2025. *FishBase* [Electronic Database]. www.fishbase.org.

Fulton, E.A., Smith, A.D.M., Smith, D.C., Van Putten, I.E., 2011. Human behaviour: the key source of uncertainty in fisheries management. Fish Fish. 12 (1), 2–17. https://doi.org/10.1111/j.1467-2979.2010.00371.x.

Ganias, K., Somarakis, S., Koutsikopoulos, C., Machias, A., 2007. Factors affecting the spawning period of sardine in two highly oligotrophic seas. Mar. Biol. 151, 1559–1569. https://doi.org/10.1007/s00227-006-0601-0.

Garrido, S., Marçalo, A., Zwolinski, J., Van der Lingen, C., 2007. Laboratory investigations on the effect of prey size and concentration on the feeding behaviour of *Sardina pilchardus*. Mar. Ecol. Prog. Ser. 330, 189–199. https://doi.org/10.3354/meps330189.

Gkanasos, A., Schismenou, E., Tsiaras, K., Somarakis, S., Giannoulaki, M., Sofianos, S., Triantafyllou, G., 2021. A three-dimensional; full life cycle; anchovy and sardine model for the North Aegean Sea (eastern Mediterranean): validation; sensitivity and climatic scenario simulations. Mediterr. Mar. Sci. 22 (3), 653–668. https://doi.org/10.12681/mms.27407.

Grbec, B., Dulčić, J., Morović, M., 2002. Long-term changes in landings of small pelagic fish in the eastern Adriatic: possible influence of climate oscillations over the northern hemisphere. Climate Res. 20 (3), 241–252. https://doi.org/10.3354/cr020241.

Green, B.S., 2008. Maternal effects in fish populations. Adv. Mar. Biol. 54, 1–105.

Grimm, V., 2020. The ODD protocol: an update with guidance to support wider and more consistent use. Ecol. Model. 428, 109105. https://doi.org/10.1016/j.ecolmodel.2020.109105.

Haase, K., Reinhardt, O., Lewin, W.C., Weltersbach, M.S., Strehlow, H.V., Uhrmacher, A. M., 2023. Agent-based simulation models in fisheries science. Rev. Fish. Sci. Aquac. 31 (3), 372–395. https://doi.org/10.1080/23308249.2023.2201635.

Haberle, I., Bavčević, L., Klanjscek, T., 2023. Fish condition as an indicator of stock status: insights from condition index in a food-limiting environment. Fish Fish. 24 (4), 567–581. https://doi.org/10.1111/faf.12744.

Hilborn, R., Walters, C.J., 1992. Quantitative Fisheries Stock Assessment: Choice; Dynamics and Uncertainty. Chapman and Hall.

Houde, E.D., 2016. Recruitment variability. In: Jakobsen, T., Fogarty, M.J., Megrey, B.A., Moksness, E. (Eds.), Fish Reproductive Biology. Wiley. https://doi.org/10.1002/9781118752739.ch3.

Jager, T., Goussen, B., Gergs, A., 2023. Using the standard DEB animal model for toxicokinetic–toxicodynamic analysis. Ecol. Model. 475, 110187. https://doi.org/10.1016/j.ecolmodel.2022.110187.

Johnson, D.W., Hixon, M.A., 2011. Sexual and lifetime selection on body size in a marine fish: the importance of life-history trade-offs. J. Evol. Biol. 24 (8), 1653–1663. https://doi.org/10.1111/j.1420-9101.2011.02298.x.

Jusup, M., Sousa, T., Domingos, T., Labinac, V., Marn, N., Wang, Z., Klanjšček, T., 2017. Physics of metabolic organization. Phys. Life Rev. 20, 1–39. https://doi.org/10.1016/j.plrev.2016.09.001.

Kearney, M., Porter, W., 2009. Mechanistic niche modelling: combining physiological and spatial data to predict species' ranges. Ecol. Lett. 12 (4), 334–350. https://doi.org/10.1111/j.1461-0248.2008.01277.x.

Kell, L.T., Mosqueira, I., Grosjean, P., Fromentin, J.-M., Garcia, D., Hillary, R., Jardim, E., Mardle, S., Pastoors, M.A., Poos, J.J., Scott, F., Scott, R.D., 2007. FLR: an open-source framework for the evaluation and development of management strategies. ICES J. Mar. Sci. 64 (4), 640–646. https://doi.org/10.1093/icesjms/fsm012.

Kooijman, S.A.L.M., 2010. Dynamic Energy Budget Theory for Metabolic Organisation, Third edition. Cambridge University Press. https://doi.org/10.1017/CBO9780511805400.

Kooijman, S.A.L.M., 2020. The standard dynamic energy budget model has no plausible alternatives. Ecol. Model. 428, 109106. https://doi.org/10.1016/j.ecolmodel.2020.109106.

Kooijman, S.A.L.M., 2024. Ways to reduce or avoid juvenile-driven cycles in individual-based population models. Ecol. Model. 490, 110649. https://doi.org/10.1016/j.ecolmodel.2024.110649.

Kooijman, S.A.L.M., Sousa, T., Pecquerie, L., van der Meer, J., Jager, T., 2008. From fooddependent statistics to metabolic parameters: a practical guide to the use of dynamic energy budget theory. Biol. Rev. 83 (4), 533–552. https://doi.org/10.1111/j.1469-185x.2008.00053.x.

Kooijman, S.A.L.M., van der Hoeven, N., van der Werf, D.C., 1989. Population consequences of a physiological model for individuals. Funct. Ecol. 3, 325–336.

Kooijman, S.A.L.M., Pecquerie, L., Augustine, S., Jusup, M., 2011. Scenarios for acceleration in fish development and the role of metamorphosis. J. Sea Res. 66, 419–423. https://doi.org/10.1016/j.seares.2011.08.001.

Leonori, I., Ticina, V., Giannoulaki, M., Hattab, T., Iglesias, M., Bonanno, A., Costantini, I., Canduci, G., Machias, A., Ventero, A., Somarakis, S., Tsagarakis, K., Bogner, D., Barra, M., Basilone, G., Genovese, S., Juretić, T., Gašparević, D., De Felice, A., 2021. History of hydroacoustic surveys of small pelagic fish species in the European Mediterranean Sea. Mediterr. Mar. Sci. 22 (4 Suppl), 751–768. https://doi.org/10.12681/mms.26001.

Libralato, S., Coll, M., Tempesta, M., Santojanni, A., Spoto, M., Palomera, I., Arneri, E., Solidoro, C., 2010. Food-web traits of protected and exploited areas of the Adriatic Sea. Biol. Conserv. 143 (9), 2182–2194. https://doi.org/10.1016/j.biocon.2010.06.002.

Libralato, S., Celic, I., Serpetti, N., Agnetta, D., Panzeri, D., Reale, M., Cossarini, G., Solidoro, C., Ricci, P., Cipriano, G., Carlucci, R., Vrgoc, N., Isajlovic, I., Scarcella, G., Masnadi, F., Angelini, S., Miokovic, D., Krstulović Šifner, S., Labanchi, L., Russo, T., D'Andrea, L., 2020. Deliverable D4.7.1: Calibrated Ecopath with Ecosim model for the Adriatic and Ionian region [Technical report]. FAIRSEA – Fisheries in the Adriatic Region: A Shared Ecosystem Approach (Interreg Italy–Croatia). https://programming14-20.italy-croatia.eu/documents/273958/0/FAIRSEA_D4.7.1_food_web_model_v1.pdf.

Lika, K., Kearney, M.R., Freitas, V., van der Veer, H.W., van der Meer, J., Wijsman, J.W.M., Pecquerie, L., Kooijman, S.A.L.M., 2011. The "covariation method" for estimating the parameters of the standard dynamic energy budget model I: philosophy and approach. J. Sea Res. 66 (4), 270–277. https://doi.org/10.1016/j.seares.2011.07.010.

Lindkvist, E., Wijermans, N., Daw, T.M., González-Mon, B., Giron-Nava, A., Johnson, A.F., van Putten, I., Basurto, X., Schlüter, M., 2020. Navigating complexities: agent-based modeling to support research; governance; and management in small-scale fisheries. Front. Mar. Sci. 6, 733. https://doi.org/10.3389/fmars.2019.00733.

Marano, G., Casavola, N., Rizzi, E., De Ruggieri, P., Lo Caputo, S., 1998. Valutazione delle risorse pelagiche; consistenza dello stock di sardine e alici nell'Adriatico meridionale. Anni 1984–1996. Biol. Mar. Mediterr. 5, 313–320.

Marchal, P., De Oliveira, J.A.A., Lorance, P., Baulier, L., Pawlowski, L., 2013. What is the added value of including fleet dynamics processes in fisheries models? Can. J. Fish. Aquat. Sci. 70 (7), 992–1010. https://doi.org/10.1139/cjfas-2012-0326.

Marques, G.M., Augustine, S., Lika, K., Pecquerie, L., Domingos, T., Kooijman, S.A.L.M., 2018. The AmP project: comparing species on the basis of dynamic energy budget parameters. PLoS Comput. Biol. 14, e1006100. https://doi.org/10.1371/journal.pcbi.1006100.

Marshall, D.J., Barneche, D.R., White, C.R., 2022. How does spawning frequency scale with body size in marine fishes? Fish Fish. 23 (2), 316–323. https://doi.org/10.1111/faf.12617.

Martin, B.T., Zimmer, E.I., Grimm, V., Jager, T., 2012. Dynamic energy budget theory meets individual-based modelling: a generic and accessible implementation. Methods Ecol. Evol. 3 (5), 445–449. https://doi.org/10.1111/j.2041-210X.2011.00168.x.

Menu, C., 2024. Population Dynamics and Evolution of Biological Traits of Anchovy and Sardine in the Bay of Biscay: A Coupled DEB-IBM Approach. Doctoral dissertation. *Univ*, Bretagne Occidentale. https://tel.archives-ouvertes.fr/tel-04871292.

Menu, C., Pecquerie, L., Bacher, C., Doray, M., Hattab, T., van der Kooij, J., Huret, M., 2023. Testing the bottom-up hypothesis for the decline in size of anchovy and sardine across European waters through a bioenergetic modeling approach. Prog. Oceanogr. 210, 102943. https://doi.org/10.1016/j.pocean.2022.102943.

Morello, E.B., Arneri, E., 2009. Anchovy and sardine in the Adriatic Sea — an ecological review. Oceanogr. Mar. Biol. Annu. Rev. 47, 209–256.

Mustać, B., Cukar, G.Z., Vidović, A., 2020. Comparison of growth parameters between sardine *Sardina pilchardus* (Walbaum; 1792) and anchovy *Engraulis encrasicolus* (Linnaeus; 1758) from the eastern Adriatic Sea. J. Marit. Transp. Sci. 3, 325–333.

Nespeca, V., Comes, T., Brazier, F., 2023. A methodology to develop agent-based models for policy support via qualitative inquiry. J. Artif. Soc. Soc. Simul. 26 (1), 10. https://doi.org/10.18564/jasss.5014.

Nisbet, R.M., Jusup, M., Klanjscek, T., Pecquerie, L., 2012. Integrating dynamic energy budget (DEB) theory with traditional bioenergetic models. J. Exp. Biol. 215 (6), 892–902. https://doi.org/10.1242/jeb.059675.

Nunes, C., Marques, G., Sousa, T., Kooijman, B., Queirós, Q., Lefebvre, S., Donati, E., 2025. AmP *Sardina pilchardus*; Version 2025/02/07. Add-my-Pet database.

Palomera, I., Olivar, M.P., Salat, J., Sabatés, A., Coll, M., García, A., Morales-Nin, B., 2007. Small pelagic fish in the NW Mediterranean Sea: an ecological review. Prog. Oceanogr. 74, 377–396. https://doi.org/10.1016/j.pocean.2007.04.012.

Parry, H.R., Bithell, M., 2012. Large scale agent-based modelling: A review and guidelines for model scaling. In: Heppenstall, A., Crooks, A., See, L., Batty, M. (Eds.), Agent-Based Models of Geographical Systems. Springer, pp. 271–308. https://doi.org/10.1007/978-90-481-8927-4_14.

Pauly, D., Christensen, V., Walters, C., 2000. Ecopath; Ecosim; and Ecospace as tools for evaluating ecosystem impact of fisheries. ICES J. Mar. Sci. 57, 697–706. https://doi.org/10.1006/jmsc.2000.0726.

Pecquerie, L., Kooijman, B., 2015. AmP *Engraulis encrasicolus*; Version 2015/09/21. Add-my-Pet database.

Pecquerie, L., Petitgas, P., Kooijman, S.A.L.M., 2009. Modeling fish growth and reproduction in the context of the dynamic energy budget theory to predict environmental impact on anchovy spawning duration. J. Sea Res. 62 (2–3), 93–105. https://doi.org/10.1016/j.seares.2009.06.002.

Pedersen, M.W., Berg, C.W., 2017. A stochastic surplus production model in continuous time. Fish Fish. 18 (2), 226–243. https://doi.org/10.1111/faf.12174.

Pethybridge, H., Bodin, N., Arsenault-Pernet, E.J., Bourdeix, J.H., Brisset, B., Bigot, J.L., Roos, D., Peter, M., 2014. Temporal and interspecific variations in forage fish feeding conditions in the NW Mediterranean: lipid content and fatty acid compositional changes. Mar. Ecol. Prog. Ser. 512, 39–54. https://doi.org/10.3354/meps10864.

Politikos, D., Somarakis, S., Tsiaras, K.P., Giannoulaki, M., Petihakis, G., Machias, A., Triantafyllou, G., 2015. Simulating anchovy's full life cycle in the northern Aegean Sea (eastern Mediterranean): a coupled hydro-biogeochemical–IBM model. Prog. Oceanogr. 138, 399–416. https://doi.org/10.1016/j.pocean.2014.09.002.

Postel, L., Fock, H., Hagen, W., 2000. ICES Zooplankton Methodology Manual. Elsevier.

Punt, A.E., 2023. Those who fail to learn from history are condemned to repeat it: a perspective on current stock assessment good practices and the consequences of not following them. Fish. Res. 261, 106642. https://doi.org/10.1016/j.fishres.2023.106642.

Punt, A.E., Dalton, M.G., Cheng, W., Hermann, A.J., Holsman, K.K., Hurst, T.P., Ianelli, J.N., Kearney, K.A., McGilliard, C.R., Pilcher, D.J., Veron, M., 2021. Evaluating the impact of climate and demographic variation on future prospects for fish stocks: an application for northern rock sole in Alaska. Deep-Sea Res. II Top. Stud. Oceanogr. 189–190, 104951.

Queirós, Q., Fromentin, J.-M., Gasset, E., Dutto, G., Huiban, C., Metral, L., Leclerc, L., Schull, Q., McKenzie, D.J., Saraux, C., 2019. Food in the sea: size also matters for pelagic fish. Front. Mar. Sci. 6, 385. https://doi.org/10.3389/fmars.2019.00385.

Railsback, S.F., Grimm, V., 2011. Agent-Based and Individual-Based Modeling: A Practical Introduction. Princeton University Press.

Regner, S., 1985. Ecology of planktonic stages of the anchovy; *Engraulis encrasicolus* (Linnaeus; 1758); in the central Adriatic. Acta Adriat. 26 (1), 5–113.

Regner, S., Piccinetti Manfrin, G., Piccinetti, C., 1988. The spawning of the sardine (*Sardina pilchardus* Walb.) in the Adriatic as related to the distribution of temperature. FAO Fish. Rep. 39, 127–132.

Ricklefs, R.E., Wikelski, M., 2002. The physiology/life-history nexus. Trends Ecol. Evol. 17 (10), 462–468. https://doi.org/10.1016/S0169-5347(02)02578-8.

Roesch, E., Greener, J.G., MacLean, A.L., Nassar, H., Rackauckas, C., Holy, T.E., Stumpf, M.P.H., 2023. Julia for biologists. Nat. Methods 20 (5), 655–664. https://doi.org/10.1038/s41592-023-01832-z.

Rose, K.A., Allen, J.I., Artioli, Y., Barange, M., Blackford, J., Carlotti, F., Cropp, R., Daewel, U., Edwards, K., Flynn, K., Hill, S.L., HilleRisLambers, R., Huse, G., Mackinson, S., Megrey, B., Moll, A., Rivkin, R., Salihoglu, B., Schrum, C., Zhou, M., 2010. End-to-end models for the analysis of marine ecosystems: challenges; issues; and next steps. Mar. Coast. Fish. 2 (1), 115–130. https://doi.org/10.1577/C09-059.1.

Rose; K. A.; Fiechter; J.; Curchitser; E. N.; Hedstrom; K.; Bernal; M.; Creekmore; S.; Haynie; A.; Ito; S.-i.; Lluch-Cota; S.; Megrey; B. A.; Edwards; C. A.; Checkley; D.; Koslow; T.; McClatchie; S.; Werner; F.; MacCall; A.; & Agostini; V. 2015. Demonstration of a fully coupled end-to-end model for small pelagic fish using sardine and anchovy in the California current. Prog. Oceanogr.; 138; 348–380. doi: https://doi.org/10.1016/j.pocean.2015.01.012.

Rose, K.A., Holsman, K., Nye, J.A., Markowitz, E.H., Banha, T.N.S., Bednaršek, N., Bueno-Pardo, J., Deslauriers, D., Fulton, E.A., Huebert, K.B., Huret, M., Ito, S., Koenigstein, S., Li, L., Moustahfid, H., Muhling, B.A., Neubauer, P., Paula, J.R., Siddon, E.C., Skogen, M.D., Spencer, P.D., van Denderen, P.D., van der Meeren, G.I., Peck, M.A., 2024. Advancing bioenergetics-based modeling to improve climate change projections of marine ecosystems. Mar. Ecol. Prog. Ser. 732, 193–221. https://doi.org/10.3354/meps14535.

Sæther, B.-E., Coulson, T., Grøtan, V., Engen, S., Altwegg, R., Armitage, K.B., Barbraud, C., Becker, P.H., Blumstein, D.T., Dobson, F.S., Festa-Bianchet, M., Gaillard, J.-M., Jenkins, A., Jones, C., Nicoll, M.A.C., Norris, K., Oli, M.K., Ozgul, A., Weimerskirch, H., 2013. How life history influences population dynamics in fluctuating environments. Am. Nat. 182 (6), 743–759. https://doi.org/10.1086/673497.

Salonen, K., Sarvala, J., Hakala, I., Viljanen, M.-L., 1976. The relation of energy and organic carbon in aquatic invertebrates. Limnol. Oceanogr. 21, 724–730.

Schwartzlose, R.A., Alheit, J., Bakun, A., Baumgartner, T.R., Cloete, R., Crawford, R.J.M., Fletcher, W.J., Green-Ruiz, Y., Hagen, E., Kawasaki, T., Lluch-Belda, D., Lluch-Cota, S.E., MacCall, A.D., Matsuura, Y., Nevárez-Martínez, M.O., Parrish, R.H., Roy, C., Serra, R., Shust, K.V., Zuzunaga, J.Z., 1999. Worldwide large-scale fluctuations of sardine and anchovy populations. S. Afr. J. Mar. Sci. 21, 289–347. https://doi.org/10.2989/025776199784125962.

Shin, Y.-J., Rochet, M.-J., Jennings, S., Field, J.G., Gislason, H., 2005. Using size-based indicators to evaluate the ecosystem effects of fishing. ICES J. Mar. Sci. 62 (3), 384–396. https://doi.org/10.1016/j.icesjms.2005.01.004.

Sinovčić, G., 1986. Estimation of growth; mortality; production and stock size of sardine; *Sardina pilchardus* (Walb.); from the middle Adriatic. Acta Adriat. 27, 67–74.

Sinovčić, G., Zorica, B., 2006. Reproductive cycle and minimal length at sexual maturity of *Engraulis encrasicolus* (L.) in the Zrmanja River estuary (Adriatic Sea; Croatia). Estuar. Coast. Shelf Sci. 69, 439–448.

Somarakis, S., Palomera, I., Garcia, A., Quintanilla, L., Koutsikopoulos, C., Uriarte, A., Motos, L., 2004. Daily egg production of anchovy in European waters. ICES J. Mar. Sci. 61, 944–958. https://doi.org/10.1016/j.icesjms.2004.07.018.

Thunell, V., Gårdmark, A., Huss, M., Vindenes, Y., 2023. Optimal energy allocation trade-off driven by size-dependent physiological and demographic responses to warming. Ecology 104 (4), e3967. https://doi.org/10.1002/ecy.3967.

van der Meer, J., 2006. An introduction to dynamic energy budget (DEB) models with special emphasis on parameter estimation. J. Sea Res. 56 (2), 85–102. https://doi.org/10.1016/j.seares.2006.03.001.

van der Meer, J., Hin, V., van Oort, P., van de Wolfshaar, K.E., 2022. A simple DEB-based ecosystem model. Conserv. Physiol. 10 (1), coac057. https://doi.org/10.1093/conphys/coac057.

Verberk, W.C.E.P., Atkinson, D., Hoefnagel, K.N., Hirst, A.G., Horne, C.R., Siepel, H., 2021. Shrinking body sizes in response to warming: explanations for the temperature-size rule with special emphasis on the role of oxygen. Biol. Rev. 96 (1), 247–268. https://doi.org/10.1111/brv.12653.

Véron, M., Duhamel, E., Bertignac, M., Pawlowski, L., Huret, M., Baulier, L., 2020. Determinism of temporal variability in size at maturation of sardine *Sardina pilchardus* in the Bay of Biscay. Front. Mar. Sci. 7. https://doi.org/10.3389/fmars.2020.567841.

Vichi, M., Lovato, T., Butenschön, M., Tedesco, L., Lazzari, P., Cossarini, G., Masina, S., Pinardi, N., Solidoro, C., Zavatarelli, M., 2023. The Biogeochemical Flux Model (BFM): Equation Description and User Manual (Version 5.3; Report Series no. 1; Release 1.3). BFM community. http://bfm-community.eu.

Walker, N.D., Boyd, R., Watson, J., Kotz, M., Radford, Z., Readdy, L., Sibly, R., Roy, S., Hyder, K., 2020. A spatially explicit individual-based model to support management of commercial and recreational fisheries for European sea bass *Dicentrarchus labrax*. Ecol. Model. 431, 109179. https://doi.org/10.1016/j.ecolmodel.2020.109179.

Watson, J.W., Boyd, R., Dutta, R., Vasdekis, G., Walker, N.D., Roy, S., Everitt, R., Hyder, K., Sibly, R.M., 2022. Incorporating environmental variability in a spatially-explicit individual-based model of European sea bass. Ecol. Model. 466, 109878. https://doi.org/10.1016/j.ecolmodel.2022.109878.

Zorica, B., Čikeš Keč, V., Pešić, A., Gvozdenović, S., Kolitari, J., Mandić, M., 2019. Spatiotemporal distribution of anchovy early life stages in the eastern Adriatic Sea in relation to some oceanographic features. J. Mar. Biol. Assoc. U. K. 99 (5), 1205–1211. https://doi.org/10.1017/S0025315418001145.